Journal of
Molluscan Studies

The Malacological Society of London

Journal of Molluscan Studies (2024) **90**: eyad027. https://doi.org/10.1093/mollus/eyad027
Published online 8 February 2024

Variability in the white spot: a new genus and species of Discodorididae (Nudibranchia) from the central and western Pacific Ocean

Samantha A. Donohoo [1,2] and Terrence M. Gosliner [1,2]

[1]*Department of Invertebrate Zoology and Geology, California Academy of Sciences, 55 Music Concourse Drive, San Francisco, CA 94118, USA; and*
[2]*Department of Biology, San Francisco State University, 1600 Holloway Avenue, San Francisco, CA 94132, USA*

Correspondence: S.A. Donohoo; e-mail: sdonohoo@calacademy.org

urn:lsid:zoobank.org:pub:7A71A6AD-1A8B-49AD-ABAC-21D9411311EC

(Received 30 August 2022; editorial decision 12 June 2023)

ABSTRACT

In this paper, a new genus in the nudibranch family Discodorididae, *Avaldesia* n. gen., is established for *Avaldesia albomacula* (Chan & Gosliner, 2007) and *Avaldesia tahala* (Chan & Gosliner, 2007), originally assigned to the genus *Thordisa* Bergh, 1877, and a new species, *Avaldesia tamatoa* n. sp., described here from the central Pacific. To establish species relationships within *Avaldesia*, as well as the placement of *Avaldesia* within Discodorididae, we utilized four molecular markers (cytochrome *c* oxidase subunit I, 16S rRNA, histone H3 and 28S rRNA) in our Bayesian inference and maximum likelihood analyses. Four species delimitation methods were complemented by morphological dissections and scanning electron microscopy. Our results reveal a clear separation between *Avaldesia* and *Thordisa* and suggest that *Avaldesia* is more closely related to the genera *Hoplodoris* Bergh, 1880 and *Asteronotus* Ehrenberg, 1831. The most characteristic features of *Avaldesia* include a radula with increasing denticulation towards the fimbriate outermost laterals and a reproductive system with a lobate vestibular gland, occasional hollow vestibular spine and a penis armed with one or more penial spines. All species of *Avaldesia* are found in shallow water (5–10 m depth) on rocky reefs, sandy sediments and algal fields with distributions across the Indo-Pacific.

INTRODUCTION

The Discodorididae is a family of cryptobranch nudibranch sea slugs that can retract their gill into a gill pocket and prey upon a wide variety of sponges in almost every marine ecosystem in the world (Alvim & Pimenta, 2013). The original description of Discodorididae included 10 genera (Bergh, 1891); however, this would later expand to 22 after Valdés (2002) synonymized 16 families/subfamilies under Discodorididae in a morphological phylogenetic review of all cryptobranch genera. To date, the family Discodorididae is currently composed of 29 recognized genera and *c.* 200+ described species (MolluscaBase eds, 2021); however, the diversity and systematics of the entire family have yet to be fully explored. Previous systematic studies within Discodorididae have relied on morphology to establish new species and their corresponding relationships within individual genera (Fahey & Gosliner, 1999, 2001, 2003; Garovoy *et al.*, 2001; Chan & Gosliner, 2006, 2007; Camacho-García & Gosliner, 2008; Padula & Valdés, 2012). More recent studies have begun utilizing both morphological and molecular data to establish the evolutionary history and relationships within genera and support new species descriptions (Fahey, 2003; Lindsay *et al.*, 2016; Tibiriçá *et al.*, 2018, 2023; Donohoo & Gosliner, 2020; Neuhaus *et al.*, 2021; Innabi *et al.*, 2023).

The genus *Thordisa* was originally described based on the type species *Thordisa maculigera* Bergh, 1877, which was later synonymized with *T. villosa* (Alder & Hancock, 1864) based on similarities in the dorsum colouration, tubercule arrangement and the radular teeth, including the presence of "pectinate outermost lateral teeth". *Thordisa* has previously been suggested to be a monophyletic genus in prior morphological studies (Valdés, 2002; Chan & Gosliner, 2006, 2007); however, Donohoo & Gosliner (2020) found that *Thordisa* was a polyphyletic genus with two distinct clades during re-establishment of the genus *Hoplodoris* Bergh, 1880a. The first clade included *T. bimaculata* Lance, 1966, which grouped together with specimens of *Geitodoris* Bergh, 1891; *Discodoris* Bergh, 1877; and *Carminodoris* Bergh, 1889. The second clade included specimens of *Thordisa* aff. *albomacula* representing three distinct species (labelled clades A–C), which were suggested to be the closest relative to *Hoplodoris* and *Asteronotus* Ehrenberg, 1831.

In this paper, we further explore the three species previously identified in the second clade of supposed *Thordisa* species and propose a new genus *Avaldesia*, with *Avaldesia albomacula* (Chan & Gosliner, 2007) as the type species. Our analyses include additional representatives of *Thordisa* and *Avaldesia* from the central and eastern Pacific and the Mediterranean, including the Marshall

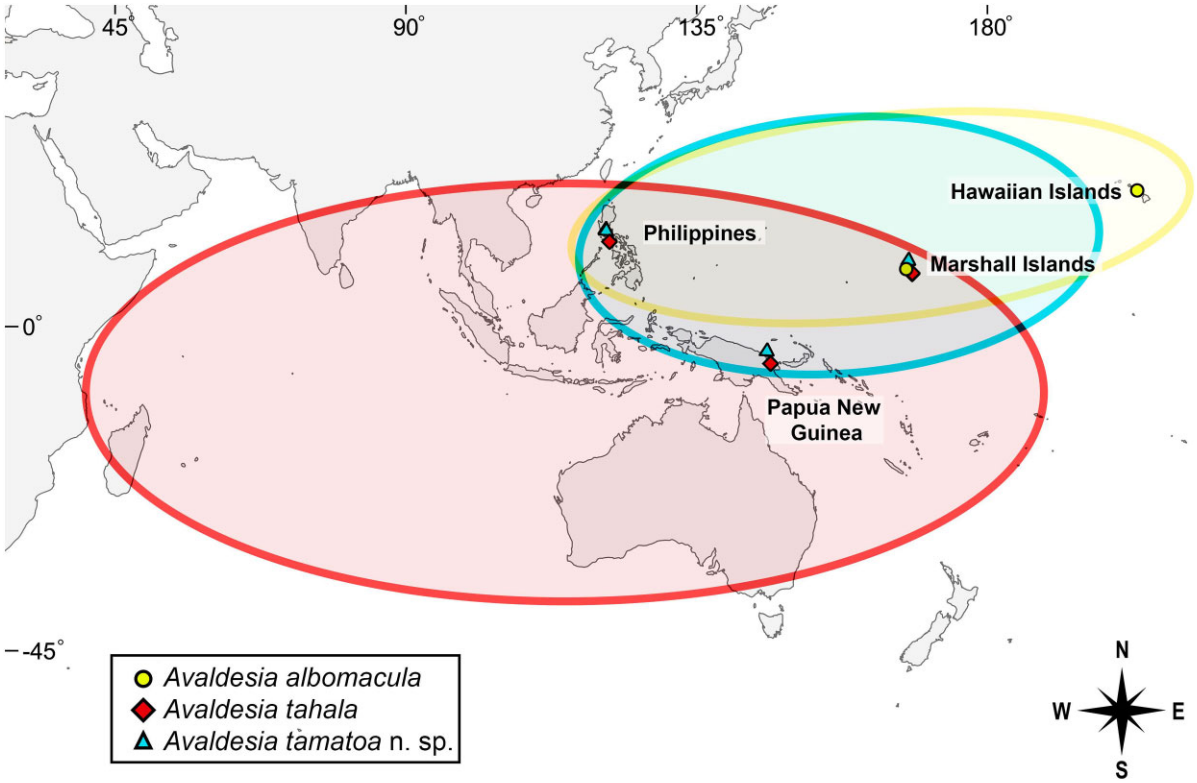

Figure 1. Map of the localities sampled for this study coloured by species with estimates of geographic range based on published literature and this study.

Islands, Papua New Guinea, the Philippines, Mexico and Morocco. We provide further detailed descriptions for the previously described species *A. albomacula* and *A. tahala* (Chan & Gosliner, 2007), as well as a description for the new species *A. tamatoa* n. sp. described from the central and eastern Pacific.

MATERIAL AND METHODS

Taxon sampling

All specimens used for sequencing in this study were originally collected for molecular sequencing and preserved in 95% ethanol. Sixteen specimens representing two previously described species (*Avaldesia albomacula* and *A. tahala*) and one new species (*A. tamatoa* n. sp.), collected from the central and western Pacific Ocean (Fig. 1), were sequenced for this study. A total of 57 specimens, 16 newly sequenced and 31 with two or more genes previously published on GenBank, were used in the molecular analyses. Sequenced specimens, voucher numbers, localities and GenBank accession numbers are listed in Table 1. Goniodorididae, Doridiidae and several members of Discodorididae were used for outgroup comparisons based on the molecular phylogenetic analyses by Hallas *et al.* (2017) and Donohoo & Gosliner (2020). Voucher specimens and holotypes are deposited in the collections at the California Academy of Sciences (CASIZ), San Francisco, California, USA.

DNA extraction, amplification and sequencing

DNA was extracted from a small sample of each specimen's foot or mantle using a Qiagen Dneasy Blood and Tissue Kit (Qiagen, Valencia, CA, USA). Fragments from four genes, mitochondrial cytochrome *c* oxidase I (COI) and 16S ribosomal RNA (16S rRNA) and nuclear histone 3 (H3) and 28S ribosomal RNA (28S rRNA), were used to estimate our *Avaldesia* phylogeny based on previous sequencing success for members of Discodorididae including *Asteronotus*; *Diaulula* Bergh, 1878; *Halgerda* Bergh, 1880b; *Hoplodoris*; *Jorunna* Bergh, 1876; and *Thordisa* (Fahey, 2003; Giribet *et al.*, 2006; Göbbeler & Klussmann-Kolb, 2010; Lindsay *et al.*, 2016; Hallas *et al.*, 2017; Tibiriçá *et al.*, 2018; Donohoo & Gosliner, 2020; Neuhaus *et al.*, 2021; Innabi *et al.*, 2023; Tibiriçá *et al.*, 2023). Each polymerase chain reaction (PCR) used gene-specific primers (Table 2) and contained the following: 2.5 μl of 10 × PCR buffer, 0.5 μl dNTPs (10 mM stock), 0.5 μl of each primer (10 μM stock), 0.25 μl DreamTaq^{TM} Hot Start DNA Polymerase (5 U/μl, Thermo Fisher), 5 μl betaine, 2 μl bovine serum albumin, 2–4 μl of template DNA, and then filled to a final volume of 25 μl with Millipore-H_2O. In both 28S rRNA PCRs, an additional 1 μl of dimethyl sulfoxide was added to account for secondary structure and nucleotide repeats. The PCR gene-specific protocols followed Donohoo & Gosliner (2020) and were run on a BioRad MyCycler Thermocycler (Bio-Rad Laboratories) at the California Academy of Sciences Center for Comparative Genomics (CCG). The amplified DNA was stained with ethidium bromide and examined using gel electrophoresis on a 1% TBE agarose gel. Successfully amplified products were cleaned using an ExoSAP-IT protocol (USB Scientific). In samples with bold bands, 2 μl of ExoSAP-IT was added to 5 μl of PCR product, while in samples with weaker bands, 1 μl of ExoSAP-IT was added to 7 μl of PCR product. The clean double-stranded products were then sequenced in the CCG or at the Museo Nacional de Ciencias Naturales of Madrid (Madrid, Spain) or ELIM Biopharmaceuticals (Hayward, CA, USA). In the CCG, the cleaned PCR products were fluorescently labelled with dye terminators (Big Dye 3.1, Applied Biosystems) during cycle sequencing, which followed the SteP protocol (Platt *et al.*, 2007). Each cycle sequencing reaction contained: 1.5 μl of 5 × reaction buffer, 0.3 μl of primer (10 mM stock), 0.75 μl of Big Dye, 4.45–5.45 μl of Millipore-H_2O and 2–3 μl of cleaned PCR product.

Table 1. Voucher, locality and GenBank accession numbers for specimens successfully sequenced and dissected.

Species	Voucher	Locality	GenBank acc. nos			
			16S rRNA	28S rRNA	COI	H3
Outgroup species						
Ancula gibbosa	CASIZ 182028	Cape Elizabeth, Maine, USA	KP340291	KP340356	KP340388	KP340413
Aphelodoris sp. 1	CASIZ 176920	Oudekraal, South Africa	MF958293	MF958379	MF958424	–
Asteronotus cespitosus	CASIZ 177226	Balayan Bay, Philippines	KP871680	MN728188	KP871633	KP871656
Asteronotus cespitosus	CASIZ 191321	Madang Province, Papua New Guinea	MN722443	MN728203	MN720296	MN720327
Asteronotus hepaticus	CASIZ 191310	Madang, Papua New Guinea	MN722442	MN728202	MN720295	MN720326
Asteronotus markaensis	CASIZ 192316A	Marka Island, Saudi Arabia	MN722446	MN728206	MN720299	MN720330
Asteronotus mimeticus	CASIZ 208221	Verde Island, Philippines	MN722452	MN728211	MN720305	MN720336
Asteronotus namuro	CASIZ 192297	Tigerhead Island, Saudi Arabia	MN722445	MN728205	MN720298	MN720329
Asteronotus spongicolus	CASIZ 192317A	Kaust Beach, Saudi Arabia	MN722447	MN728207	MN720300	MN720331
Asteronotus spongicolus	CASIZ 194597	Maricaban Island, Philippines	MN722448	MN728208	MN720301	MN720332
Asteronotus spongicolus	CASIZ 227581	Barracuda Point, Tanzania	MN722454	MN728213	MN720307	MN720338
Atagema notacristata	CASIZ 167980	Isla Uva, Panama	KP871681	MT452661	KP871634	KP871657
Carminodoris flammea	CASIZ 177628	Calumpan Peninsula, Philippines	MN722433	MN728190	MN720285	MN720311
Diaulula sandiegensis	CASIZ 181321	Scott Creek, California, USA	MN722435	MN728193	MN720287	MN720317
Discodoris boholiensis	CASIZ 204802	Puerto Galera, Philippines	MN722451	MN728210	MN720304	MN720335
Geitodoris heathi	CASIZ 181314	Carmel Point, California, USA	KP871690	MN728192	KP871642	KP871666
Halgerda dalanghita	CASIZ 200578	Maricaban Island, Philippines	MW220902	MW220141	MW223040	MW414966
Hoplodoris desmoparypha	CASIZ 70066	Okinawa, Japan	MN722431	MN728185	MN720283	MN720309
Hoplodoris desmoparypha	CASIZ 309550	Ngermutidech, Palau	MN722455	–	MN720308	–
Hoplodoris rosans	CASIZ 182837	Calumpan Peninsula, Philippines	MN722436	MN728195	MN720288	MN720318
Hoplodoris rosans	CASIZ 182921	Calumpan Peninsula, Philippines	MN722438	MN728197	MN720290	MN720320
Paradoris liturata	CASIZ 182756	Maricaban Strait, Philippines	MW220951	MW220191	MW223084	MW415015
Peltodoris nobilis	CASIZ 182223	Pillar Point, California, USA	HM162593	MN728194	HM162684	HM162499
Platydoris sanguinea	CASIZ 177762	Maricaban Island, Philippines	MF958285	MF958372	MF958416	MN720312
Rostanga byga	CASIZ 181157	Devonshire Parish, Bermuda	MW220952	MW220192	MW223085	MW415016
Rostanga elandsia	CASIZ 176110	Olifantsbos Bay, South Africa	KP871699	MN728187	KP871651	KP871674
Sclerodoris sp.	CASIZ 179945	Airport Beach, Hawaii, USA	OL964389	OL964405	OL960075	OL956540
Sclerodoris sp.	CASIZ 182866	Balayan Bay, Philippines	MN722437	MN728196	MN720289	MN720319
Sclerodoris sp.	CASIZ 182894	Maricaban Island, Philippines	OL964391	OL964407	OL960077	OL956542
Sclerodoris sp.	CASIZ 185093	Legan Island, Marshall Islands	OL964392	OL964408	OL960078	OL956543
Sclerodoris sp.	CASIZ 191525	Madang, Papua New Guinea	MN722444	MN728204	MN720297	MN720328
Sclerodoris sp.	CASIZ 193515	Kwajalein Atoll, Marshall Islands	OL964400	OL964416	–	OL956551
Sclerodoris tuberculata	CASIZ 190788	Madang, Papua New Guinea	MF958286	MF958373	MF958417	MN720323
Taringa aivica	CASIZ 186481A	Punta Rosarito, Mexico	OL964394	OL964410	OL960080	OL956545
Taringa sp.	CASIZ 172039	Tortuga, Ecuador	MN722432	MN728186	MN720284	MN720310
Taringa telopia	CASIZ 182933	Bocas Del Toro, Panama	KP871700	MN728198	MN720291	KP871675
Thordisa azmanii	MNCN: ADN 151079	Aghroud, Morocco	OR096359	–	OR088279	OR089094
Thordisa bimaculata	CASIZ 184516	Naples, California, USA	MN722439	MN728199	MN720292	MN720321
Thordisa oliva	CASIZ 181139	Bigej-Meck Reef, Marshall Islands	OL964390	OL964406	OL960076	OL956541
Thordisa cf. *nieseni*	CASIZ 173057	Islas Marietas, Mexico	MW220954	MW220194	MW223087	MW415018
Thordisa sanguinea	CASIZ 182457	Mabini, Philippines	OQ359121	OQ359122	OQ357898	OQ368830
Ingroup species						
Avaldesia albomacula	CASIZ 181136	Bigej-Meck Reef, Marshall Islands	MN722434	MN728191	MN720286	MN720314
Avaldesia albomacula	CASIZ 220322	Maalaea Bay, Hawaii, USA	MT452884	OL964419	MT454620	MT454624
Avaldesia tahala	CASIZ 177688	Maricaban Island, Philippines	MT452886	MT452657	–	MT454626
Avaldesia tahala	CASIZ 181345	Bigej-Meck Reef, Marshall Islands	MT452885	MT452656	MT454621	MT454625
Avaldesia tahala	CASIZ 190785	Cement Mixer Reef, Papua New Guinea	OL964395	OL964411	–	OL956546
Avaldesia tahala	CASIZ 190821	Tabad Island, Papua New Guinea	MT452887	MT452658	–	MT454627
Avaldesia tahala	CASIZ 191562	Madang Province, Papua New Guinea	OL964397	OL964413	–	OL956548
Avaldesia tahala	CASIZ 191572	Madang Province, Papua New Guinea	OL964398	OL964414	–	OL956549
Avaldesia tahala	CASIZ 208650	Puerto Galera, Philippines	OL964402	OL964418	–	OL956553
Avaldesia tamatoa n. sp.	CASIZ 179586	Bigej-Meck Reef, Marshall Islands	MT452889	MT452660	MT454623	MT454629
Avaldesia tamatoa n. sp.	CASIZ 179590	Bigej-Meck Reef, Marshall Islands	MF958287	MF958374	MF958418	MN720313

Table 1. Continued

Species	Voucher	Locality	GenBank acc. nos			
			16S rRNA	28S rRNA	COI	H3
Avaldesia tamatoa n. sp.	CASIZ 182834	Balayan Bay, Philippines	MT452888	MT452659	MT454622	MT454628
Avaldesia tamatoa n. sp.	CASIZ 185767	Bigej-Meck Reef, Marshall Islands	OL964393	OL964409	OL960079	OL956544
Avaldesia tamatoa n. sp.	CASIZ 191276	Madang Province, Papua New Guinea	OL964396	OL964412	–	OL956547
Avaldesia tamatoa n. sp.	CASIZ 193496	North Loi Island, Marshall Islands	OL964399	OL964415	OL960081	OL956550
Avaldesia tamatoa n. sp.	CASIZ 194007	Bigej-Meck Reef, Marshall Islands	OL964401	OL964417	OL960082	OL956552

Species names represent current proposed taxonomy. Dashes indicate missing sequences.

Table 2. Primers for DNA amplification and relevant Bayesian substitution models.

Primer	Sequence	Source	Substitution model	Length (bp)	Codon position
16S rRNA			GTR + I + G	459	
AR	5′-CGCCTGTTTATCAAAAACAT-3′	Palumbi *et al.* (1991)			
BR	5′-CCGGTCTGAACTCAGATCACGT-3′	Palumbi *et al.* (1991)			
28S rRNA			GTR + I + G	833	
D2	5′-CTTGGTCCGTGTTTCAAGACGG-3′	Dayrat *et al.* (2001) (modified)			
C1'	5′-ACCCGCTGAATTTAAGCAT-3′	Dayrat *et al.* (2001)			
C2'	5′-GAAAGAACTTTGAAGAGAGAGTTCA-3′	Dayrat *et al.* (2001) (modified)			
C2	5′-TGAACTCTCTCTTCAAAGTTCTTTTC-3′	Dayrat *et al.* (2001)			
COI			GTR + I + G	219	P1
HCO2198	5′-TAAACTTCAGGGAGACCAAAAAATCA-3′	Folmer *et al.* (1994)	GTR + I + G	219	P2
LCO1490	5′-GGTCAACAAATCATAAAGATATTGG-3′	Folmer *et al.* (1994)	HKY + I + G	220	P3
H3			GTR + I + G	109	P1
AF	5′-ATGGCTCGTACCAAGCAGACVGC-3′	Colgan *et al.* (1998)	JC + I	109	P2
AR	5′-ATATCCTTRGGCATRATRGTGAC-3′	Colgan *et al.* (1998)	HKY + G	110	P3

The newly labelled single-strand DNA was precipitated using 2.5 μl of EDTA followed by washing and centrifugation with 100% and 70% ethanol, respectively. Any residual ethanol was evaporated in a 60 °C incubator before adding 10 μl of HiDi formamide (Applied BioSystems). DNA was then denatured at 95 °C for 2 min, cooled on ice and then sequenced on an ABI3130 Genetic Analyzer.

Sequence alignment and phylogenetic analyses

Both directions of each successful gene fragment were assembled, trimmed to remove primers and then edited as necessary using Geneious v. 11.1.5 (Kearse *et al.*, 2012) and Mesquite v. 3.51 (Maddison & Maddison, 2018). Each sequence was checked for contamination using the BLAST function within Geneious. Individual gene alignments were aligned with MAFFT v. 1.5.0 (Katoh *et al.*, 2009) using the algorithm E-INS-I. Additional editing for 16S rRNA and 28S rRNA alignments was done by hand. The protein-coding genes COI and H3 regions were translated into amino acids in Mesquite using the invertebrate mitochondrial code and checked for stop codons. Bayesian inference (BI) and maximum likelihood (ML) analyses were used to evaluate the evolutionary relationships within *Avaldesia*. Single-gene alignments were independently analysed before being concatenated into a four-gene (COI + 16S rNA + H3 + 28S rRNA) alignment. Best-fit evolution models were determined using PartitionFinder2 (Lanfear *et al.*, 2017). The single-gene and concatenated datasets were each partitioned by gene and/or codon position for both the BI and ML analyses (Table 2). BI was performed in MrBayes v. 3.2.7a (Ronquist & Huelsenbeck, 2003) with 5×10^7 generations, Markov chains sampled every 1,000 generations, and the standard 25% burn-in calculated. Convergence of the two chains was checked using TRACER v. 1.7.1 (Drummund & Rambaut, 2007). A 50% majority rule consensus tree of calculated posterior probabilities (PPs) was created from the remaining tree estimates with tree branches considered strongly supported if PP values were $\geq$0.95, while values $\leq$0.94 were considered to have low support (Alfaro *et al.*, 2003). RAxML v. 8.2.12 (Stamatakis, 2014) was used with the evolution model GTR + GAMMA + I to estimate nonparametric bootstrap (BS) values and was set for 5×10^4 fast bootstrap runs. Branches with BSs of $\geq$70 were considered strongly supported, while those with values $\leq$70 were considered weakly supported (Alfaro *et al.*, 2003).

Species delimitation analyses

Species were delimited using four different approaches: (1) automatic barcode gap discovery (ABGD) method (Puillandre *et al.*, 2012), (2) assemble species by automatic partitioning (ASAP) method (Puillandre *et al.*, 2021), (3) Bayesian Poisson tree process (bPTP; Zhang *et al.*, 2013) and (4) general mixed Yule coalescent (GMYC) model (Pons *et al.*, 2006; Fujisawa & Barraclough, 2013). The ABGD method detects breaks between intraspecific and interspecific species variation using genetic pairwise distance. An ingroup COI alignment and an ingroup 16S rRNA alignment created in Mesquite were uploaded to the ABGD web-based interface (https://bioinfo.mnhn.fr/abi/public/abgd/abgdweb.html). To evaluate which settings were congruent with our molecular and morphological analyses, we tested Jukes–Cantor (JC69), Kimura (K80) and simple distances for each ingroup

to evaluate which parameters were congruent with our phylogenetic and morphological analyses (Supplementary Material Figs S1 and S2; Kekkonen *et al.*, 2015; Tibiriçá *et al.*, 2018). The following parameters were applied for both ingroups: Jukes–Cantor (JC69): *P*.min = 0.001; *P*.max = 0.1; steps = 10; NB = 20 with a relative gap width × = 1.5.

The ASAP method is similar to the ABGD method; however, it does not rely on an *a priori* species hypothesis, and it provides a scoring system to assist with choosing an accurate partition scheme. The previously created COI and 16S rRNA ingroup alignments were uploaded to the ASAP web-based interface (https://bioinfo.mnhn.fr/abi/public/asap/asapweb.html) and run using the setting Jukes–Cantor (JC69). Bayesian PTP identifies groups descended from a common ancestor by modelling the number of substitutions between branches in a previously inputted Bayesian phylogenetic tree. The bPTP analysis was performed using the four gene concatenated BI tree (outgroup pruned) on the bPTP server with the following parameters: 100,000 generations, 100 thinning, 0.1 burn-in and 123 seeds. Convergence was checked using the ML convergence plot generated by the bPTP server.

The GMYC model assumes that species evolved independently and that the diversification between species results in different branching rates that can be delimited using the Yule model (Fujisawa & Barraclough, 2013). An ultrametric COI tree was estimated using BEAST v. 1.10.4 with the following priors defined in BEAUTi v. 1.10.4: GTR + GAMMA + I, Yule speciation process, uncorrelated lognormal relaxed clock, 10 million generations and MCMC chain length sampled every 1,000 steps. Run convergence was checked using TRACER v. 1.7.1. A maximum clade credibility tree was created in TreeAnnotator v. 1.10.4 after removing the first 10% of trees (i.e. burnin). The GMYC approach was performed in R v. 4.2.1 using the R package Species Limits by Threshold Statistics (SPLITS, v. 1.0–20; Fujisawa & Barraclough, 2013) and the "single threshold" model (Pons *et al.*, 2006). Branch support was evaluated using bootstrap support (BS) and Bayesian PP values.

Morphological analysis

External morphological features were examined and described utilizing photographs of living animals and when necessary preserved specimens. Representatives of each species were dissected along the foot using a Nikon SMZ-U dissection microscope. The reproductive system and buccal mass were removed and then hand-drawn using a camera lucida drawing attachment on a Nikon SMZ-U dissection microscope. The buccal mass was then dissolved in 10% sodium hydroxide (NaOH) for 12–24 h. The remaining labial cuticle and radula were rinsed with deionized water and mounted for examination by scanning electron microscope (SEM). In the reproductive system of *A. tamatoa* n. sp., the vestibular spines and penial spines were dissected from the vestibular gland and penis, respectively, and then mounted for SEM imaging. Due to their small size, the vestibular spines and penial spines of *A. albomacula* and *A. tahala* were soaked in 75% ethanol mixed with acid fuchsin stain and then sequentially rinsed in 95% ethanol, 100% ethanol and xylene before being permanently mounted on glass microscope slides for examination. The SEM samples were coated with gold/palladium using a Cressington 108 Auto vacuum sputter coater, and micrographs were taken using a Hitachi SU3500 SEM at CASIZ. Specimens and the corresponding dissected structures were deposited in the collection of the Department of Invertebrate Zoology (CASIZ) collection.

RESULTS

Phylogenetic analyses

Fifty-eight new sequences were published on GenBank with the following accession numbers: COI (OL960075−OL960082, OQ357898 and OR088279), 16S rRNA (OL964389−OL964402, OQ359121 and OR096359), H3 (OL956540−OL956553, OQ368830 and OR089094) and 28S rRNA (OL964405−OL964419 and OQ359122). The final concatenated dataset was 2,278 bp, including gaps, while the single-gene alignments were 658, 459, 328 and 833 bp for COI, 16S rRNA, H3 and 28S rRNA, respectively. Not all four genes were successfully sequenced for all specimens, and occasionally partial sequences were obtained and used for analyses (Table 1). The single-gene trees (Supplementary Material Figs S5–S8) generally yielded poorer resolution in comparison to the four-gene concatenated tree (Fig. 2).

The COI phylogenetic analyses reveal a lack of support for *Avaldesia* (PP = 0.70, BS = 59); however, the species and relationships within *Avaldesia* are all well supported (PP = 1, BS > 75; Supplementary Material Fig. S5). The 16S rRNA phylogenetic analyses reveal some well-supported groupings as seen in *Avaldesia albomacula* (PP = 1, BS = 100) and *A. tamatoa* n. sp. (PP = 1, BS = 96); however, *A. tahala* is not supported in the BI analysis but is well supported in the ML analysis (PP = 0.85, BS = 77). The relationships within *Avaldesia* in the 16S rRNA trees are also unsupported (PP < 0.90, BS < 60; Supplementary Material Fig. S6). The H3 phylogenetic analyses are largely unresolved with only *A. albomacula* successfully grouping together (PP = 0.96, BS = 96); while individual specimens of *A. tahala* and *A. tamatoa* n. sp. share a large polytomy with the *A. albomacula* group and the majority of the outgroup (Supplementary Material Fig. S7). The 28S rRNA phylogenetic analyses is semi-resolved with strong support for *Avaldesia* (PP = 0.99, BS = 86), *A. albomacula* (PP = 1, BS = 97) and *A. tamatoa* n. sp. (PP = 0.99, BS = 79); however, one specimen of *A. tahala* (CASIZ 208650) fails to group with the other six specimens of *A. tahala*. In the 28S rRNA trees, the rest of *A. tahala* is unsupported in the BI analysis but well supported in the ML analysis (PP = 0.63, BS = 88; Supplementary Material Fig. S8).

The BI and ML four-gene analyses support *Avaldesia* as a distinct genus within the family Discodoridiidae (PP = 1, BS = 99). In this study and in Donohoo & Gosliner (2020), a clade composed of *Hoplodoris* and *Asteronotus* is well supported (PP = 1, BS = 92) as the sister taxa of *Avaldesia*. Within *Avaldesia*, the previously described species *A. albomacula* (PP = 1, BS = 100) is well supported (PP = 1, BS = 99) as the sister species to the previously described *A. tahala* (PP = 1, BS = 100) and the new species *A. tamatoa* n. sp. (PP = 1, BS = 100).

Species delimitation analyses

The COI ABGD analysis recovered ten partitions with each partition recovering the same three species (Supplementary Material Table S1). The 16S rRNA ABGD analysis recovered seven partitions with two partitions of six groups with a prior maximal distance smaller than 0.0017 and five partitions of three groups with a prior maximal distance greater than 0.0028 (Supplementary Material Table S2). In the 16S rRNA partitions with six groups, the new species *A. tamatoa* n. sp. is split into multiple groups; however, there are no morphological or geographical characteristics to support these groupings. Therefore, the COI and 16S rRNA partitions with three groups are the most congruent with our phylogenetic analyses. The COI and 16S rRNA ABGD genetic distances (i.e. uncorrected p-distances) are listed in Table 3.

The maximum genetic distance for COI between the three species of *Avaldesia* was 14.7% between *A. albomacula* and *A. tahala*, the minimum was 9.6% between *A. tahala* and *A. tamatoa* n. sp., and intraspecific variation was 2.9% in *A. albomacula* and 0.0–1.2% in *A. tamatoa* n. sp. Intraspecific variation was not calculated within *A. tahala* due to unsuccessful sequencing of the COI gene. The maximum genetic distance for 16S rRNA was 5.0% between *A. tamatoa* n. sp. and *A. albomacula*, the minimum was 3.0% between

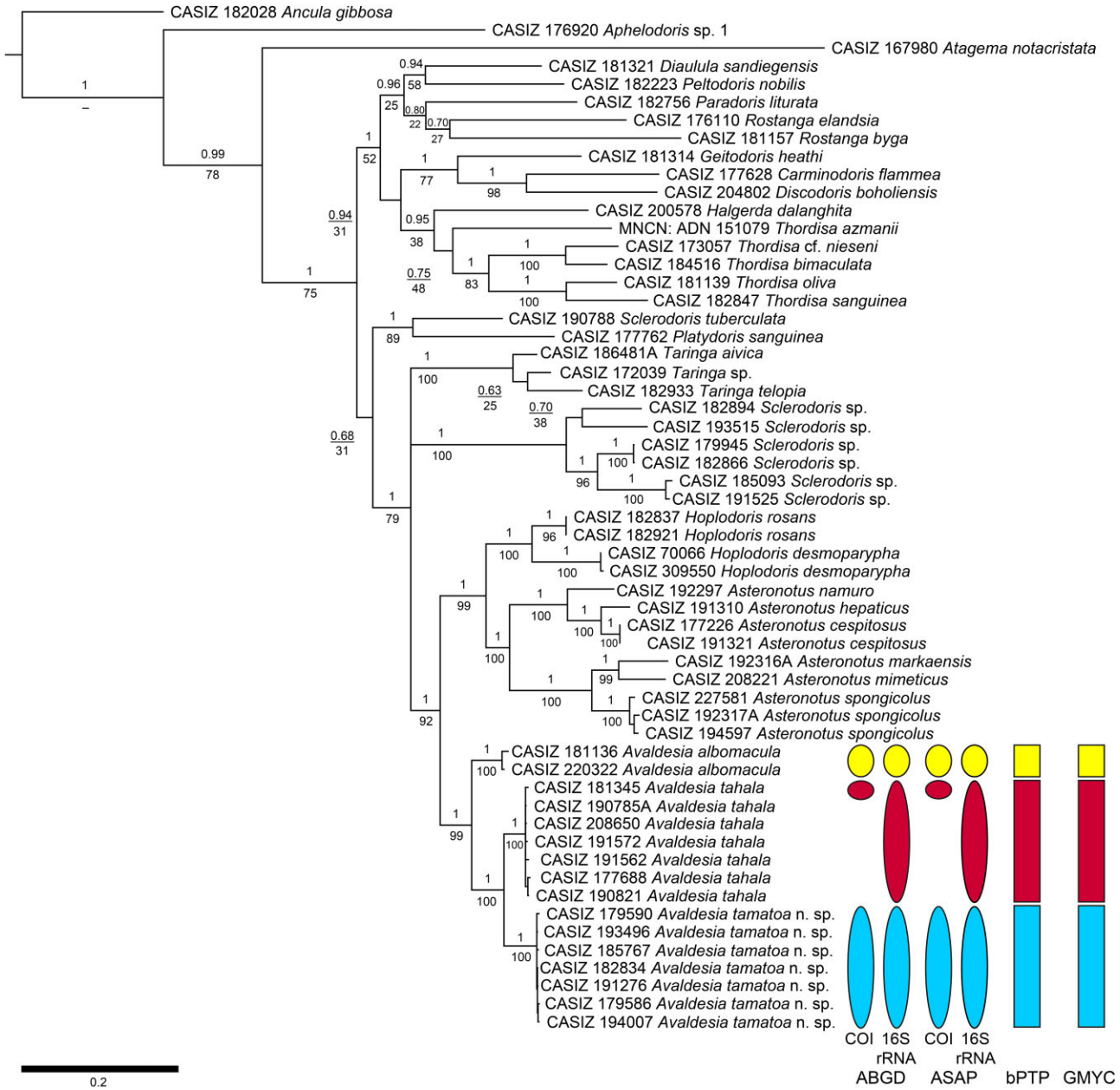

Figure 2. Bayesian phylogenetic tree of *Avaldesia* Donohoo & Gosliner n. gen. estimated from four-gene concatenated data. The numbers above and below the branches are PP and BS values, respectively; the dashes indicate relationships not recovered during the ML analysis. To the right are the 16S rRNA and cytochrome *c* oxidase I (COI) ABGD and ASAP analyses (oval) and the 16S rRNA + 28S rRNA + COI + H3 bPTP and COI GMYC analysis (square). Scale bar indicates substitutions per site.

A. albomacula and *A. tamatoa* n. sp., while intraspecific variation was 0.5% in *A. albomacula* and 0.0–0.7% in both *A. tamatoa* n. sp. and *A. tahala*.

The COI ASAP analysis (Supplementary Material Fig. S3) and the 16S rRNA ASAP analysis (Supplementary Material Fig. S4) using Jukes–Cantor (JC69) both recovered three groups (ASAP scores of 2.50 and 1.00, respectively), which are congruent with the ABGD analyses. The bPTP analysis of the four-gene concatenated dataset and the COI GMYC analysis also recovered the same three distinct groups that correspond with the ABGD, ASAP and molecular phylogenetic analyses (Fig. 2).

SYSTEMATIC DESCRIPTIONS

Superfamily Doridoidea Rafinesque, 1815
Family DISCODORIDIDAE Bergh, 1891

Genus *Avaldesia* Donohoo & Gosliner new genus

urn:lsid:zoobank.org:act:0E943090-914D-4DC8-9813-B37E5D53986E

Type species: *Avaldesia albomacula* (Chan & Gosliner, 2007)

Table 3. Pairwise uncorrected p-distances (%) for COI and 16S rRNA between *Avaldesia* spp., with intraspecific p-distances in bold.

		COI		
		1	2	3
1	*Avaldesia albomacula*	**2.9**		
2	*Avaldesia tahala*	14.2–14.7	–	
3	*Avaldesia tamatoa* n. sp.	12.0–14.0	9.6–9.9	**0.0–1.2**
		16S rRNA		
		1	2	3
1	*Avaldesia albomacula*	**0.5**		
2	*Avaldesia tahala*	3.0–3.6	**0.0–0.7**	
3	*Avaldesia tamatoa* n. sp.	4.4–5.0	3.7–4.7	**0.0–0.7**

Etymology: Named in honour of Dr Ángel Valdés, for his numerous contributions to molluscan research and his early phylogenetic work on the nudibranch family Discodoridiidae.

Diagnosis: Adult size 7–45 mm. Body shape oval. Background colour light yellow, yellow-orange, light red, deep red, reddish-purple, reddish-brown, brown, dark brown, mottled grey or dark grey. Dorsum with tan to light brown filamentous or conical papillae; short tan or white tubercles; occasionally white spots. When present, dorsum ridge pattern is low and irregular with varying complexity in each species. Rhinophores up to 9–17 lamellae with tan to brown pigment; when present, white apices. Tan to brown tripinnate gill with six branches and occasional white pigment. Foot broad; anteriorly notched, grooved. Oral tentacles digitiform. Labial cuticle smooth or armed with jaw rodlets. Radula formula 25–30 × 28–53.0.28–53. Vestigial rachidian fold present. Radular teeth hamate with increasing denticulation (1–8 denticles) especially in the middle lateral teeth. Outermost laterals reduced and semifimbriate or fimbriate. Reproductive system triaulic; ampulla large; prostate large and elongated with two distinct sections; bursa copulatrix similar sized or larger than receptaculum seminis; vestibular gland granular or fimbriate. When present, vestibular gland armed with a single hollow, hook-shaped vestibular spine. Penis armed with one to many straight or hook-shaped penial spines. Vagina unarmed.

Included species: To date, the genus is comprised of *Avaldesia albomacula* (Chan & Gosliner, 2007), *A. tahala* (Chan & Gosliner, 2007) and *A. tamatoa* n. sp., described here. It is likely that *Doris setosa* Pease, 1860, which has been included in *Thordisa* (Kay & Young, 1969), is also a species of *Avaldesia*, but its placement requires additional confirmation.

Distribution: Found on shallow reefs under coral rubble and on rocky reefs, sandy sediments and algal fields throughout the Pacific, including Madagascar (Chan & Gosliner, 2007); the Red Sea (Yonow, 2015); Indonesia (Chan & Gosliner, 2007); the Philippines (Chan & Gosliner, 2007; present study); Papua New Guinea (Chan & Gosliner, 2007; present study); Australia (Nimbs *et al.*, 2016; Nimbs & Smith, 2017); Midway Atoll (Chan & Gosliner, 2007); the Marshall Islands (Chan & Gosliner, 2007; present study); and Hawaii, USA (Chan & Gosliner, 2007; present study).

Comments: Our molecular analyses reveal that specimens previously identified as either *Thordisa albomacula* (Hallas *et al.*, 2017) or *Thordisa* aff. *albomacula* clades A–C (Donohoo & Gosliner, 2020) as well as additional representatives studied here are genetically distinct from other species of *Thordisa* studied here. Morphologically, *Thordisa* and *Avaldesia* share some external and internal characteristics (i.e. elongate dorsum tubercles, fimbriate outer radular teeth, an armed vestibular gland, etc.). However, *Avaldesia* is characterized by similarly sized inner and middle radular teeth with increasing denticulation towards the outermost radular teeth and a 'lobate' vestibular gland armed with a hollow vestibular spine.

Avaldesia albomacula (CHAN & GOSLINER, 2007) new combination

(Figs 3, 4, 5A, 6A)

Thordisa albomacula Chan & Gosliner, 2007: 292–295, figs 1C–D, 2C, 8–11. Gosliner *et al.*, 2008: 171, bottom photograph. Gosliner *et al.*, 2015: 179, top left photograph. Gosliner *et al.*, 2018: 99, top right photograph.

Type material: Holotype: CASIZ 086382, Papua New Guinea. Paratypes: seven paratypes, Papua New Guinea (CASIZ 069793, CASIZ 071206, CASIZ 072834, CASIZ 075224, CASIZ 075856, CASIZ 086414 and CASIZ 109770); one paratype, Philippines (CASIZ 083832); and one paratype, Hawaii, USA (CASIZ 109848).

Other material examined: CASIZ 181136, one specimen, dissected and sequenced, 42 mm alive, Bigej-Meck Reef (08°55′58″N 167°45′19″E), Kwajalein Atoll, Bigej-Meck Reef, Marshall Islands, Pacific Ocean, 9 m depth, 3 July 2008, collected by Jeanette Johnson. CASIZ 220322, one specimen, dissected and sequenced, 28 mm alive, Maalaea Bay (20°45′55″N 156°29′11″W), Maui, Hawaii, USA, 9–10 m depth, 1 April 2017, collected by Cory Pittman.

Diagnosis: Background colour light red, reddish-brown, dark brown, or mottled grey; dorsum with white spot anterior of gill pouch; filamentous tan papillae and occasional small white spots. Rhinophores with 12–17 lamellae with tan to brown pigment and white apices. Rhinophoral sheath smooth. Tan to brown tripinnate gill with six branches and occasional white pigment on rachises. Oral tentacles digitiform. Radular formula 26–30 × 33–53.0.33–53. Vestigial rachidian fold present. Radular teeth hamate with increasing denticulation (1–8 denticles). Outermost laterals reduced and semifimbriate/fimbriate. Labial cuticle smooth. Bursa copulatrix similar size to receptaculum seminis. Granular vestibular gland unarmed. Penis armed with numerous hook-shaped penial spines.

External morphology (Fig. 3): Body oval shaped. Living specimen length 28–42 mm. Dorsum background colouration light red, reddish-brown, dark brown or mottled grey. Small to large white spot anterior to gill pouch. Numerous filamentous tan papillae and occasional white spots dispersed across dorsum. Rhinophores perfoliate with 12–17 lamellae. Rhinophoral stalks lighter than dorsum colour, tan to brown lamellae with white apices. Rhinophoral sheath smooth. Tripinnate gill tan or brown with six branches and occasional white pigment on rachises. Foot same colour as dorsum, anteriorly notched. Oral tentacles digitiform.

Buccal armature (Fig. 4): Labial cuticle smooth, devoid of rodlets. Radular formula 30 × 53.0.53 in CASIZ 220322. Radula composed of hamate teeth with increasing denticulation towards the margins (Fig. 4A). Vestigial rachidian fold along rachis. Inner lateral teeth with one elongate denticle (Fig. 4B). Middle lateral teeth, more elongate with smaller denticles (Fig. 4C). Outer lateral teeth similar to middle laterals with more elongate denticles. Outermost two teeth small, paddle-shaped and semifimbriate (Fig. 4D).

Reproductive system (Figs 5A, 6A): Similar to reproductive system drawn and described in Chan & Gosliner (2007). Triaulic (Fig. 5A). Thin preampullary duct widens into thicker ampulla, then narrows into postampullary duct, which splits into the oviduct and short vas deferens. Vas deferens gradually expand into wider, looped granular prostate, then narrows into elongate ejaculatory portion before

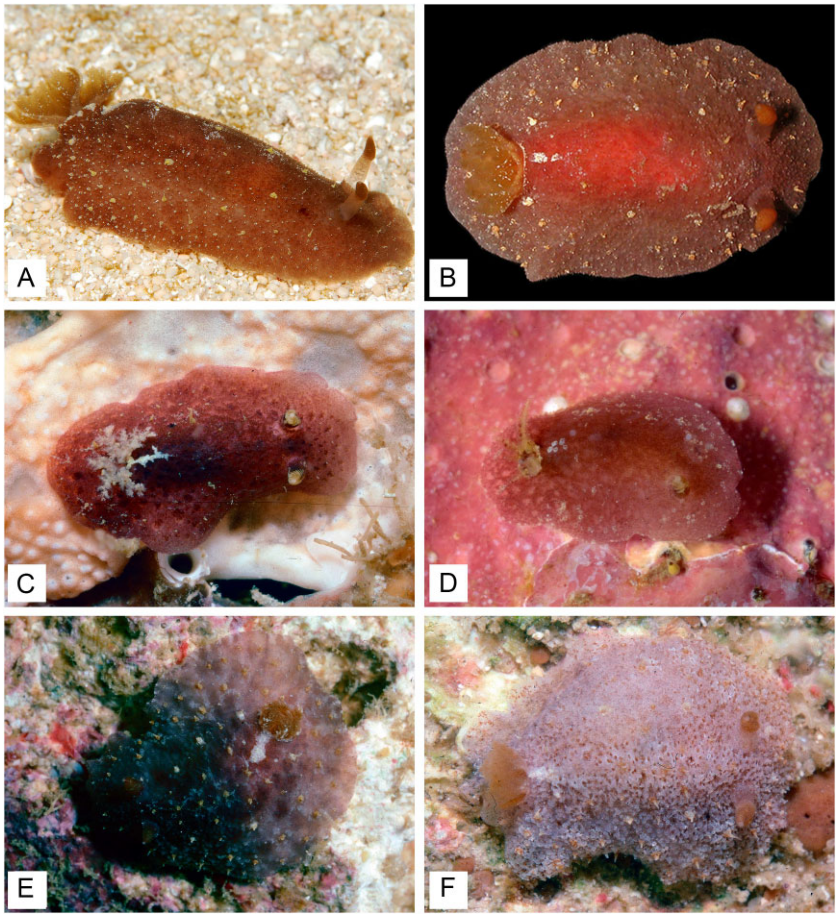

Figure 3. *Avaldesia albomacula* living animals. **A.** CASIZ 181136, Marshall Islands. **B.** CASIZ 220322, Hawaii, USA. **C.** Paratype, CASIZ 075856, Papua New Guinea. **D.** Paratype, CASIZ 083832, Philippines. **E.** Paratype, CASIZ 075224, Papua New Guinea. **F.** Paratype, CASIZ 071206, Papua New Guinea.

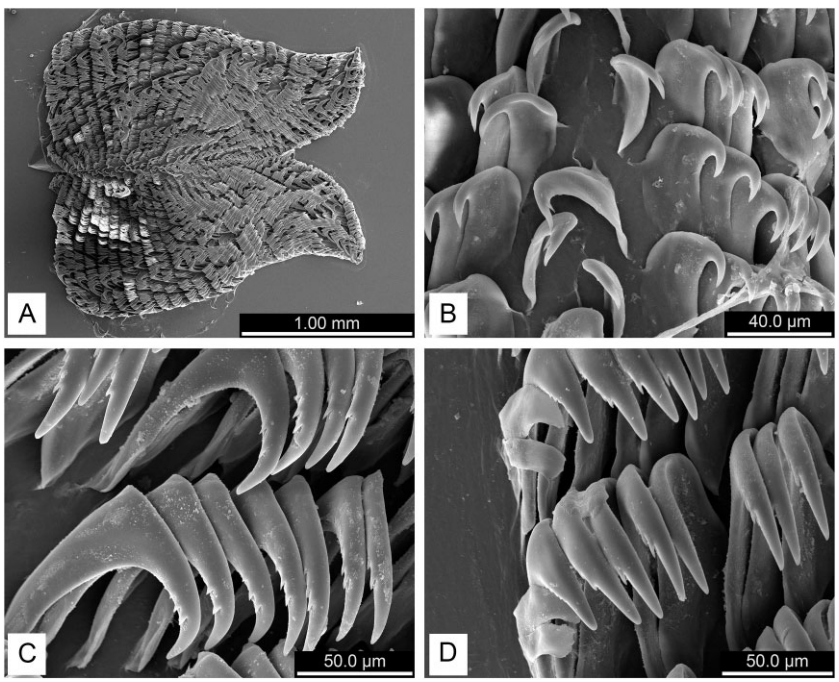

Figure 4. Radula of *Avaldesia albomacula* CASIZ 220322 (SEMs). **A.** Whole radula. **B.** Inner lateral teeth. **C.** Middle lateral teeth. **D.** Outer lateral teeth.

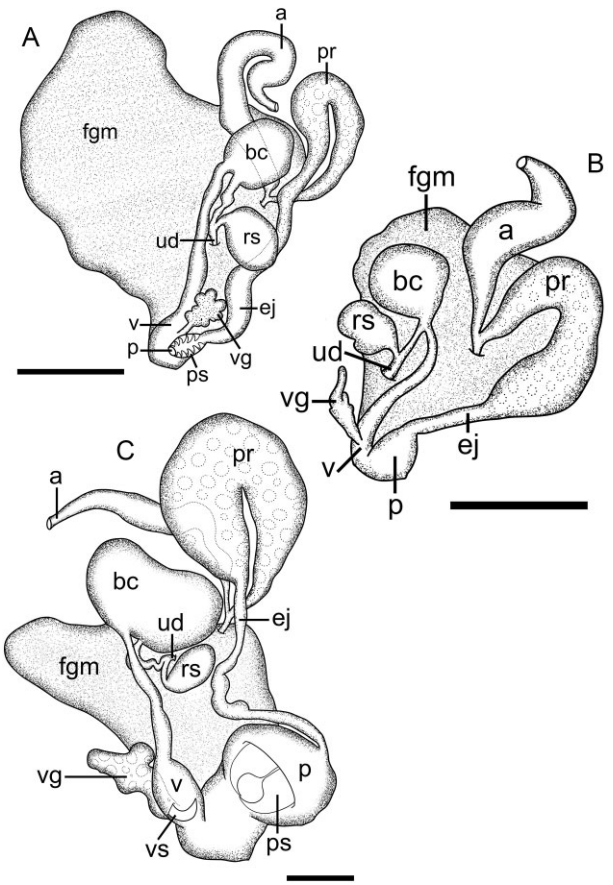

Figure 5. Reproductive system of *Avaldesia* spp. **A.** *Avaldesia albomacula* CASIZ 181136. **B.** *Avaldesia tahala* CASIZ 181345. **C.** *Avaldesia tamatoa* n. sp. holotype CASIZ 179586. Abbreviations: a, ampulla; bc, bursa copulatrix; ej, ejaculatory duct; fgm, female gland mass; p, penis; pr, prostate; ps, penial spines; rs, receptaculum seminis; ud, uterine duct; v, vagina; vg, vestibular gland; and vs, vestibular spines. Scale bars: **A** = 1 mm, **B** = 0.25 mm, **C** = 0.5 mm.

slightly expanding into penial bulb. Short, round, penis armed with numerous hook-shaped spines (Fig. 6A) and shares common genital atrium with vagina and vestibular gland. Vagina similar width to penis, proximally enters large, rounded bursa copulatrix via gradually narrowing duct. Thin, elongate duct connects bursa to slightly smaller, ovoid receptaculum seminis. Thin, short uterine duct connects between bursa and receptaculum and enters large, irregularly shaped female gland mass. Granular, vestibular gland unarmed.

Ecology: Found under coral rubble on shallow reefs 5–10 m deep (Gosliner *et al.*, 2008, 2015, 2018).

Distribution: Known from the Philippines (Chan & Gosliner, 2007); Papua New Guinea (Chan & Gosliner, 2007); the Marshall Islands (present study); and Hawaii, USA (Chan & Gosliner, 2007; present study).

Remarks: Specimens previously identified as *Thordisa* aff. *albomacula* clade A in Donohoo & Gosliner (2020) are morphologically identical to the specimens used to originally describe *Thordisa albomacula* in Chan & Gosliner (2007); however, genetically these specimens are part of a new genus, *Avaldesia*, which is clearly separated from other species of *Thordisa*. In the original description of *T. albomacula*, Chan & Gosliner (2007) noted that all specimens have similar internal anatomy (i.e. similarly sized radular teeth with increasing denticulation and fimbriate outermost teeth; a penis armed with numerous hook-shaped penial spines, etc.), but that the mantle or dorsum colour can range in colouration (reddish brown to dark grey). Chan & Gosliner (2007) also noted that all specimens of *T. albomacula* had an external white spot posterior to the gill pouch. In the two specimens studied here, we can confirm the presence of an external anterior white spot (Fig. 3A–B); however, this morphological characteristic is also found in some specimens of *A. tamatoa* n. sp. (Fig. 7C), including the former *A. albomacula* and now paratypes CASIZ 073387 and CASIZ 088385 of *A. tamatoa* n. sp. and is no longer a unique diagnostic feature for *A. albomacula*. We were also able to confirm similar anatomy between our specimens and the holotype CASIZ 086382 from Chan & Gosliner (2007), particularly the similar-sized radular teeth with increasing denticulation, as well as the presence of numerous hook-shaped penial spines. However, due to the small size of the two individuals studied here, SEM images were not captured. Instead, light microscopy was used to confirm the spines, and an updated SEM was provided for the *A. albomacula* paratype CASIZ 075856 (Fig. 6A).

In our molecular phylogeny, *A. albomacula* is sister to both *A. tamatoa* n. sp. and *A. tahala* and exhibits extremely high COI intraspecific variation (2.9%) between a specimen from the main Hawaiian Islands (CASIZ 220322) and a specimen from the Marshall Islands (CASIZ 181136). All four of our species delimitation analyses suggest that *A. albomacula* is a single species, and since the external and internal morphology of both specimens are congruent with the holotype CASIZ 086382 from Papua New Guinea, it is unlikely that the two specimens in this study represent two distinct lineages. Though uncommon, other species of nudibranchs with extremely high COI intraspecific variation, including the chromodorids *Polycera quadrilineata* (O. F. Müller, 1776) (2.4%; Sørensen *et al.*, 2020) and *Felimida binza* (Ev. Marcus & Er. Marcus, 1963) (2.89%; Padula *et al.*, 2016), the discodorid *Asteronotus spongicolus* Gosliner & Á. Valdés, 2002 (2.44%; Donohoo & Gosliner, 2020) and the sacoglossan *Thuridilla vataae* (Risbec, 1928) (3.1%; Martín-Hervás *et al.*, 2021), were each found to be a single species within their respective genera based on consistent morphological features and similar species delimitation methods utilized during this study.

Avaldesia tahala (CHAN & GOSLINER, 2007) **new combination**

(Figs 5B, 6B, 8, 9)

Thordisa tahala Chan & Gosliner, 2007: 295–299, figs 1E, 2D, 12–15. Gosliner *et al.*, 2008: 171, second photograph from the bottom. Gosliner *et al.*, 2015: 177, bottom left photograph. Yonow, 2015: 539, fig. 19. Nimbs *et al.*, 2016: 5, fig. 2C. Nimbs & Smith, 2017: 76, fig. 11D. Gosliner *et al.*, 2018: 97, bottom right photograph.

Type material: Holotype: CASIZ 71882, Madagascar. Paratypes: Madagascar (CASIZ 073252); Indonesia (CASIZ 098688); and the Marshall Islands (CASIZ 121088).

Other material examined: CASIZ 177688, one specimen, sequenced, 6 mm preserved, Bethlehem Channel, Bethlehem, Batangas Province, Philippines, 15.25 m depth, 20 April 2008, collected by T.M. Gosliner. CASIZ 181345, one specimen, dissected and sequenced, 9 mm alive, Bigej-Meck Reef (08°58′37″N 167°43′47″E), Kwajalein Atoll, Marshall Islands, Pacific Ocean, 8 m depth, 26 July 2009, collected by Jeannette Johnson. CASIZ 190785, one specimen, sequenced, 6 mm preserved, Cement Mixer Reef, Madang Province, Papua New Guinea, 6 m depth, 11 December 2012, collected by V. Knutson and J. Goodheart. CASIZ 190821, one specimen, dissected and sequenced, 6 mm preserved, Tabad Island, Madang Province, Papua New Guinea, 12 December 2012, collected by the CAS Papua New Guinea Biodiversity 2012 Expedition. CASIZ 191562, one specimen, sequenced, 5 mm preserved, Madang Province, Papua New Guinea, 6 December 2012, collected by the CAS Papua New Guinea Biodiversity

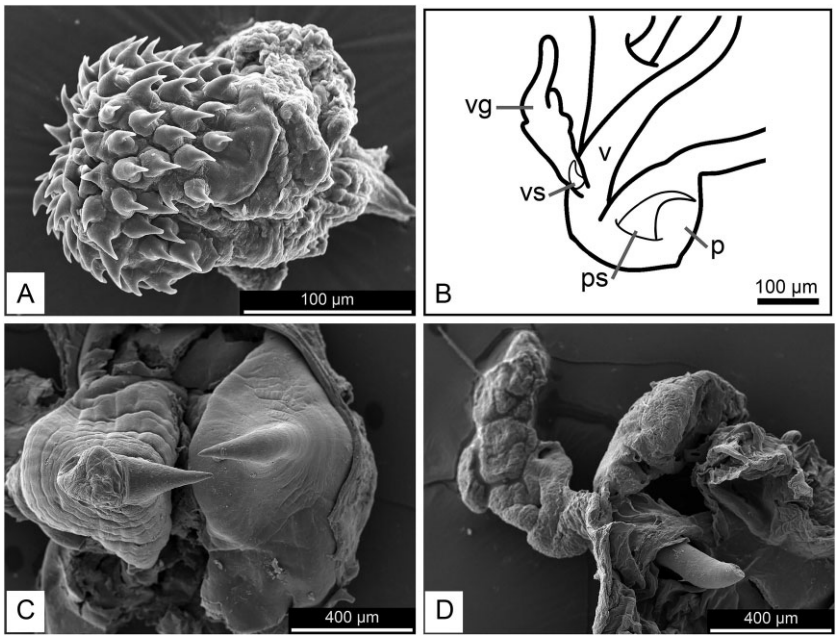

Figure 6. Penial and vestibular spine of *Avaldesia* spp. (SEMs and drawings). **A.** *Avaldesia albomacula* paratype CASIZ 075856, micrograph of penial spines. **B.** *Avaldesia tahala* CASIZ 181345, illustration of penial spine and vestibular spine. **C.** *Avaldesia tamatoa* n. sp. holotype CASIZ 179586, micrograph of penial spines. **D.** *Avaldesia tamatoa* n. sp. holotype CASIZ 179586, micrograph of vestibular spine.

2012 Expedition. CASIZ 191572, one specimen, sequenced, 3 mm preserved, Madang Province, Papua New Guinea, 6 December 2012, collected by the CAS Papua New Guinea Biodiversity 2012 Expedition. CASIZ 208650, one specimen, sequenced, 4 mm preserved, Puerto Galera (13°30′49″N 120°56′25″E), Oriental Mindoro Province, Mindoro, Philippines, 25 April 2015, collected by C.N. Piotrowski.

Diagnosis: Background colour dark grey, brown, reddish-brown or deep red; dorsal ridge network pattern low, wide, and irregular; large, conical tan papillae and short tan tubercles concentrated towards dorsum edge. Rhinophores with 9–15 lamellae, lowermost with brown pigment, uppermost with tan pigment, and white apices. Rhinophoral sheath scalloped. Tan to light brown tripinnate gill with six branches and occasional white pigment on rachises. Oral tentacles digitiform. Radular formula 25 × 28–36.0.28–36. Vestigial rachidian fold present. Radular teeth hamate with increasing denticulation (1–7 denticles). Outermost laterals reduced and fimbriate. Labial cuticle smooth. Bursa copulatrix slightly larger than receptaculum seminis. Fimbriate vestibular gland armed with one hollow hook-shaped vestibular spine. Penis armed with one straight/slightly curved spine.

External morphology (Fig. 8): Body oval shaped. Preserved specimen length 3–6 mm. Dorsum spiculose, covered with sand and particulates. Background colouration dark grey, brown, reddish-brown or deep red. Ridge network pattern low, wide and irregular. Large, conical tan papillae and short tan tubercles concentrate towards dorsum edge. Rhinophores perfoliate with 9–15 lamellae. Rhinophoral stalks same colour as dorsum, lower lamellae brown, upper lamellae tan with white apices. Rhinophoral sheath scalloped. Tripinnate gill tan or light brown with six branches and occasional white pigment on rachises. Foot same colour as dorsum, anteriorly notched. Oral tentacles digitiform.

Radula (Fig. 9): Labial cuticle smooth. Radular formula 25 × 32.0.32 in CASIZ 181345 and 25 × 29.0.29 in CASIZ 190821. Radula composed of hamate teeth with increasing denticulation towards the margins (Fig. 9A). Vestigial rachidian fold present along rachis. Inner lateral teeth with two to three denticles along short cusp (Fig. 9B). Middle lateral teeth larger, more elongate, less curved with slightly elongated denticles (Fig. 9C). Outer lateral teeth similar to middle laterals with shorter denticles. Outermost four teeth reduced and fimbriate (Fig. 9D).

Reproductive system (Figs 5B, 6B): Similar to reproductive system drawn and described in Chan & Gosliner (2007). Triaulic (Fig. 5B). Preampullary duct quickly widens into thicker ampulla, then narrows into postampullary duct, which splits into the oviduct and short vas deferens. Vas deferens expand into wider, looped granular prostate, then abruptly narrows into elongate ejaculatory portion before expanding into penial bulb. Large penis armed with one straight/slightly hooked spine (Fig. 6B) and shares common genital atrium with vagina and vestibular gland. Vagina narrower than penis proximally enters large, semirounded bursa copulatrix via gradually narrowing duct. Thin, elongate duct connects bursa to slightly smaller, ovoid receptaculum seminis. Thin, short uterine duct connects between bursa and receptaculum and enters large, irregularly shaped female gland mass. Semifimbriate vestibular gland armed with one hollow hook-shaped vestibular spine (Fig. 6B).

Ecology: Found under coral rubble and on subtidal, rocky reefs and sandy sediments *c.* 5–10 m deep (Gosliner *et al.*, 2008, 2015, 2018; Nimbs & Smith, 2017).

Distribution: Known from Madagascar (Chan & Gosliner, 2007); the Red Sea (Yonow, 2015); Indonesia (Chan & Gosliner, 2007); the Philippines (present study); Papua New Guinea (present study); Australia (Nimbs *et al.*, 2016; Nimbs & Smith, 2017); and the Marshall Islands (Chan & Gosliner, 2007; present study).

Remarks: In Chan & Gosliner's (2007) *Thordisa* morphological phylogeny, *T. albomacula* and *T. tahala* were closely related due to shared similarities in the radula (i.e. similarly sized inner and middle radular teeth and denticulation along the inner teeth) and the presence of a "lobate" vestibular gland. Our study supports that *T. albomacula* and *T. tahala* are closely related, but that both species belong to the new genus *Avaldesia* rather than *Thordisa*. Our molecular data also shows that *A. tahala* is sister to the newly described *A. tamatoa* n. sp. and that specimens previously identified as *Thordisa* aff. *Albomacula* clade B in Donohoo & Gosliner (2020) are

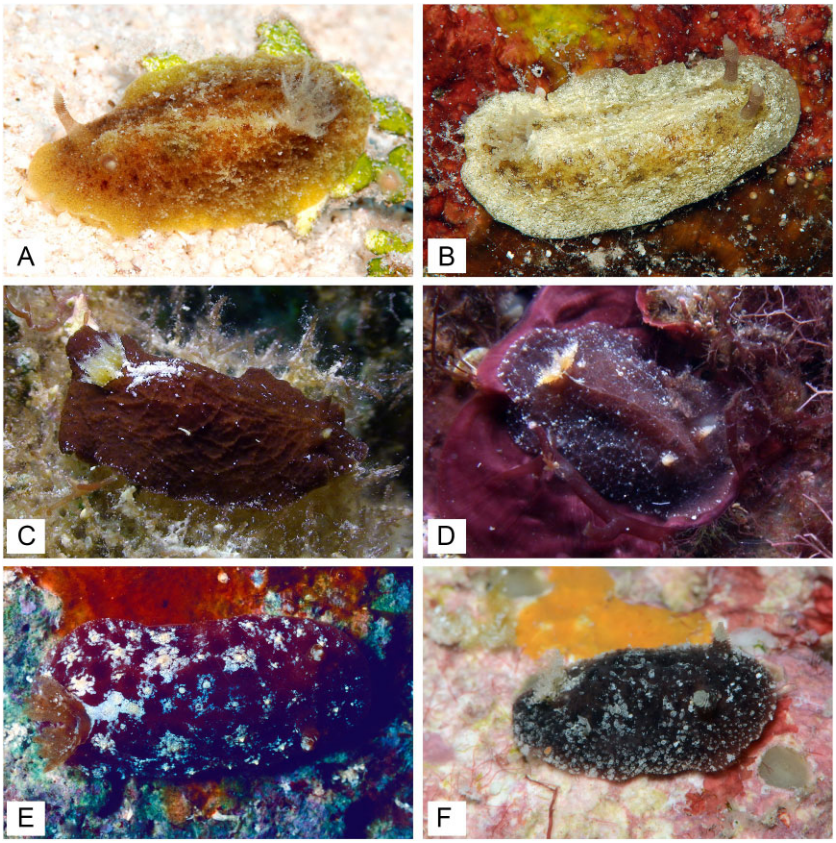

Figure 7. Living animal of *Avaldesia tamatoa* n. sp. **A.** Holotype, CASIZ 179586, Marshall Islands. **B.** Paratype, CASIZ 185767, Marshall Islands. **C.** Paratype, CASIZ 194007, Marshall Islands. **D.** Paratype, CASIZ 182834, Philippines. **E.** Paratype, CASIZ 088385, Midway Atoll. **F.** Paratype, CASIZ 193496, Marshall Islands.

morphologically and genetically identical to the additional representatives of *A. tahala* studied here. The original description of *T. tahala* includes variation in the colour of the mantle/dorsum (i.e. deep red to dark grey or brown), but individuals always presented with low dorsum ridging, increasing denticulation in the radular teeth, a single penial spine and a hollow hook-shaped vestibular spine arming a fimbriate vestibular gland (Chan and Gosliner, 2007: Figs 1E, 2D, 12–15). Our specimens, though smaller, more closely resemble the dorsum colouration (i.e. reddish-brown or dark grey) seen in the holotype CASIZ 071882 and the paratypes CASIZ 121088 and CASIZ 073252 (Fig. 9A–C) rather than the deep red seen in the Indonesian paratype CASIZ 098688. Internally, both the radula and the reproductive system of the *A. tahala* specimens dissected here are similar to those studied by Chan & Gosliner (2007). However, due to the immature size, the fimbriate nature of the vestibular gland in CASIZ 181345 is less pronounced, and the penial and vestibular spines were confirmed and then hand-drawn using light microscopy rather than SEM (Figs 5B, 6B).

***Avaldesia tamatoa* new species**

(Figs 5C, 6C–D, 7, 10)

urn:lsid:zoobank.org:act:B654BBD0-01EB-4DF6-9BBD-FF2CFC0F2520

Type material: Holotype: CASIZ 179586, one specimen, dissected and sequenced, 32 mm alive, Bigej-Meck Reef (08°55′58″N 167°45′19″E), Kwajalein Atoll, Marshall Islands, Pacific Ocean, 8 m depth, 30 August 2008, collected by Scott Johnson. Paratypes: CASIZ 073387 (formerly *T. albomacula* paratype), one specimen, dissected, 13.5 mm preserved, Madang Province, Papua New Guinea, 10 October 1986, collected by the CAS Papua New Guinea Biodiversity 1986 Expedition. CASIZ 088385 (formerly *T. albomacula* paratype), two specimens, dissected, 15–25 mm preserved, Midway Atoll, Pacific Ocean, 9.75 m depth, 29 May 1993, collected by T. M. Gosliner. CASIZ 179590, one specimen, sequenced, 26 mm alive, Bigej-Meck Reef (08°55′58″N 167°45′19″E), Kwajalein Atoll, Marshall Islands, Pacific Ocean, 7 m depth, 30 August 2008, collected by Scott Johnson. CASIZ 182834, one specimen, sequenced, 7 mm preserved, Anilao (13°44′26″N 120°53′34″E), Balayan Bay, Batangas Province, Luzon Island, Philippines, 21 May 2010, collected by Alicia Hermosillo. CASIZ 185767, one specimen, sequenced, 21 mm alive, Bigej-Meck Reef (08°55′58″N 167°45′19″E), Kwajalein Atoll, Marshall Islands, Pacific Ocean, 8 m depth, 3 April 2011, collected by Scott Johnson. CASIZ 191276, one specimen, sequenced, 7 mm preserved, Madang Province, Papua New Guinea, 16 November 2012, collected by the CAS Papua New Guinea Biodiversity 2012 Expedition. CASIZ 193496, one specimen, sequenced, 10 mm alive, North Loi Island (08°49′00″N 167°43′53″E), Kwajalein Atoll, Marshall Islands, Pacific Ocean, 5 m depth, 18 February 2013, collected by Scott Johnson. CASIZ 194007, one specimen, dissected and sequenced, 38 mm alive, Bigej-Meck Reef (08°55′40″N 167°45′27″E), Kwajalein Atoll, Marshall Islands, Pacific Ocean, 9 m depth, 13 October 2013, collected by Scott Johnson.

Etymology: Named after Tamatoa, the villainous giant crab from the Disney movie Moana due to the claw-shaped vestibular spines and the similarities between the dorsum tubercule/papillae patterning in lighter specimens and Tamatoa's extravagant shell decoration.

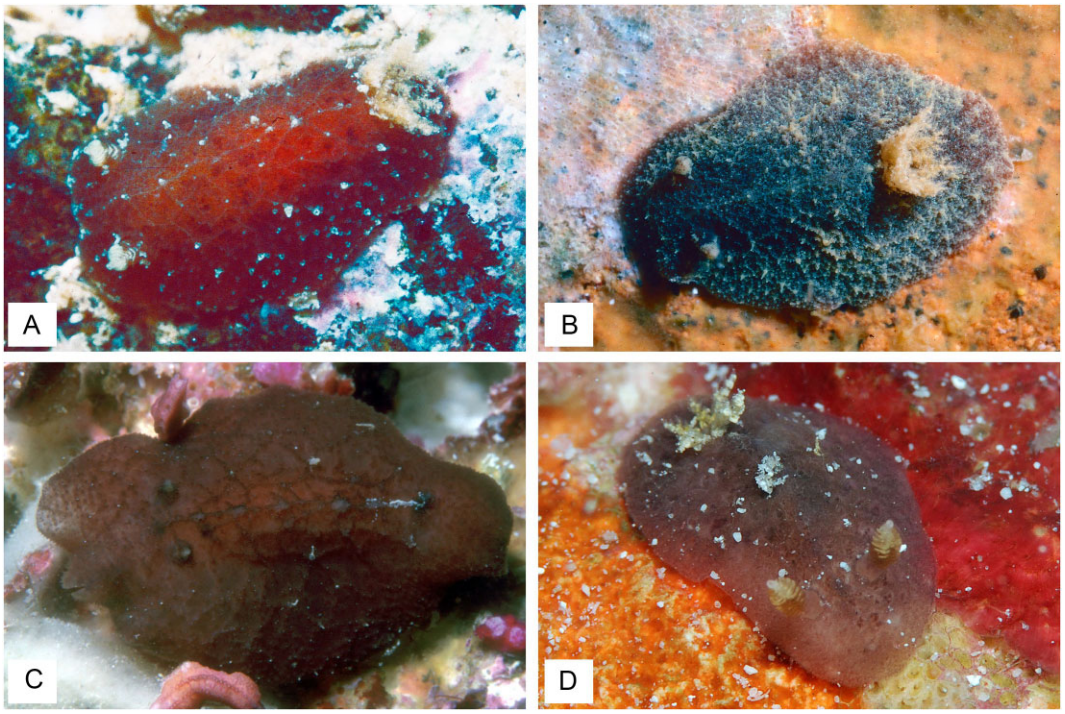

Figure 8. Living animals of *Avaldesia tahala*. **A.** Holotype, CASIZ 071882, Madagascar. **B.** Paratype, CASIZ 073252, Madagascar. **C.** Paratype, CASIZ 121088, Marshall Islands. **D.** Paratype, CASIZ 181345, Marshall Islands.

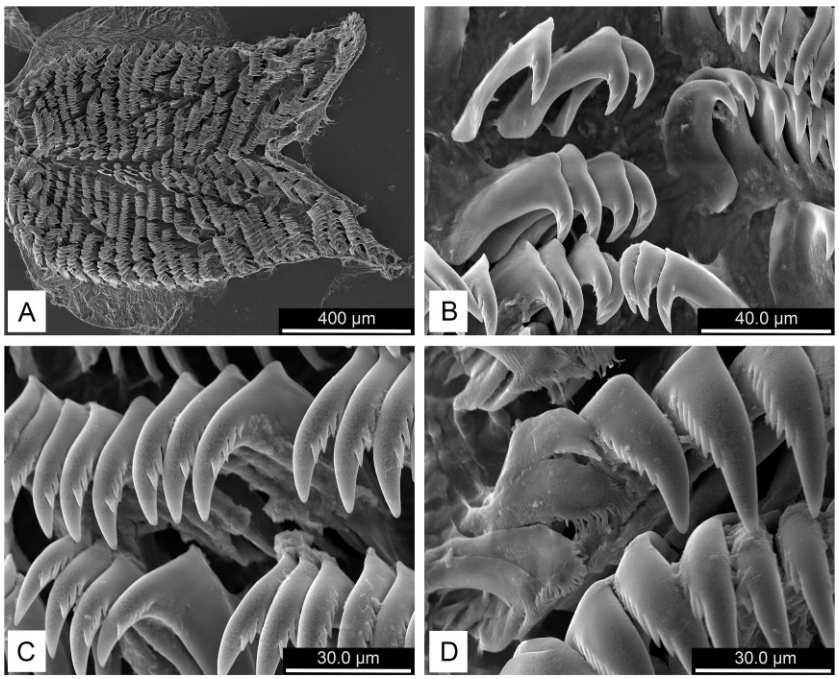

Figure 9. Radula of *Avaldesia tahala* CASIZ 181345 (SEMs). **A.** Whole radula. **B.** Inner lateral teeth. **C.** Middle lateral teeth. **D.** Outer lateral teeth.

Diagnosis: Background colour light yellow, yellow-orange, deep red, reddish-purple, or dark brown; dorsum ridge pattern low, complex and irregular; occasional, filamentous tan papillae; numerous short tan tubercles with longer white tubercles concentrated towards dorsum edge. Rhinophores with 10–13 lamellae, lowermost with brown pigment, uppermost with tan pigment and white apices. Rhinophoral sheath scalloped. Tan to light brown bipinnate, occasionally tripinnate, gill with six branches and occasional white pigment on rachises. Oral tentacles digitiform. Radular formula 28–30 × 37–43.0.37–43. Vestigial rachidian fold present. Radular teeth hamate with increasing denticulation (2–8 denticles). Outermost laterals reduced and semifimbriate. Labial cuticle armed with elongated jaw rodlets. Bursa copulatrix 2× size of receptaculum seminis. Granular vestibular gland armed with one hollow

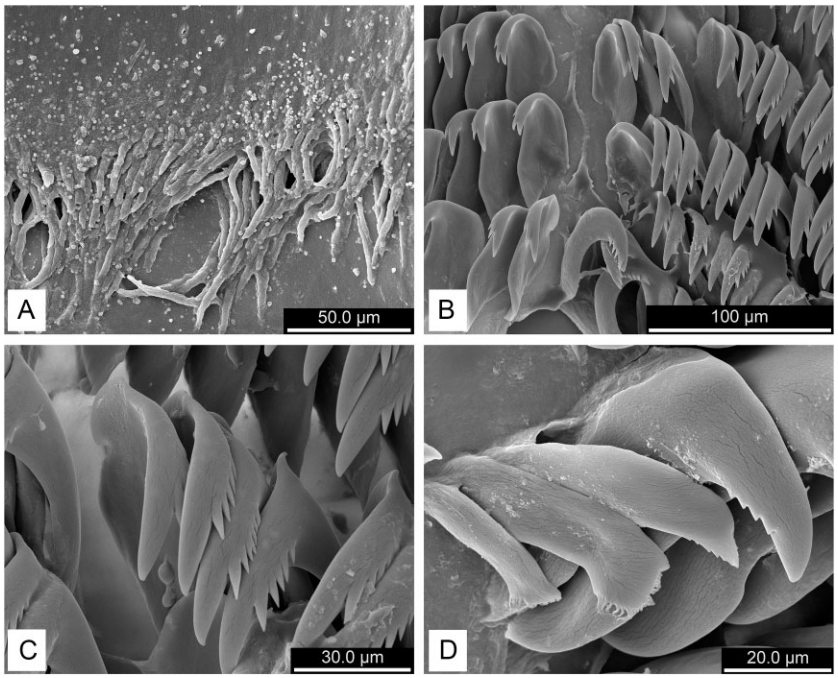

Figure 10. Radula of *Avaldesia tamatoa* n. sp. holotype CASIZ 179586 (SEMs). **A.** Jaw rodlets. **B.** Inner lateral teeth. **C.** Middle lateral teeth. **D.** Outer lateral teeth.

hook-shaped vestibular spine. Penis armed with two hook-shaped spines.

External morphology (Fig. 7): Body oval shaped. Living specimen length 10–22 mm. Dorsum occasionally covered with sand and particulates. Background colouration light yellow, yellow-orange, deep red, reddish-purple, or dark brown. Ridge pattern low, complex and irregular. Occasional filamentous tan papillae. Short tan tubercles with longer white tubercles concentrated towards dorsum edge. Rhinophores perfoliate with 10–13 lamellae. Rhinophoral stalks lighter than dorsum colour, lower lamellae brown, upper lamellae tan with white apices. Rhinophoral sheath scalloped. Bipinnate, occasionally tripinnate, gill tan or light brown with six branches and occasional white pigment on rachises. Foot same colour as dorsum, anteriorly notched. Oral tentacles digitiform.

Radula (Fig. 10): Labial cuticle armed with elongated jaw rodlets, slightly tapered with irregularly rounded tips (Fig. 10A). Radular formula 30 × 43.0.43 in holotype CASIZ 179586. Radula composed of hamate teeth with increasing denticulation towards the margins. Vestigial rachidian fold along rachis. Inner lateral teeth with two to four elongate denticles (Fig. 10B). Middle lateral teeth larger, more elongate (Fig. 10C). Outer lateral teeth similar to middle laterals with shorter cusps and shorter denticles. Outermost four teeth reduced with outer two teeth also fimbriate (Fig. 10D).

Reproductive system (Figs 5C, 6C, D): Triaulic (Fig. 5C). Thin preampullary duct widens into thicker ampulla, then narrows into postampullary duct, which splits into the oviduct and short vas deferens. Vas deferens expands into wide, looped granular prostate, then narrows into long, thin ejaculatory portion before expanding into penial bulb. Large, wide penis armed with two large, hook-shaped spines (Fig. 6C) and shares common genital atrium with vagina and vestibular gland. Vagina half the width of penis, proximally enters large, irregular bursa copulatrix via thin duct. Thin, elongate duct connects bursa to much smaller, ovoid receptaculum seminis. Thin, short uterine duct connects halfway in duct between bursa and receptaculum and enters medium-size, irregularly shaped female gland mass. Large, granular, vestibular gland armed with one hollow hook-shaped spine (Fig. 6D).

Ecology: Found under coral rubble and on subtidal, rocky reefs, sandy sediments and algal fields (particularly *Halimeda* spp. in the Marshall Islands) at *c.* 5–10 m deep.

Distribution: Known from the Philippines (present study); Papua New Guinea (Chan & Gosliner, 2007; present study); Midway Atoll (Chan & Gosliner, 2007); and the Marshall Islands (present study).

Remarks: Our molecular and species delimitation analyses reveal that specimens previously thought to be either *T. albomacula* (Chan and Gosliner, 2007) or *Thordisa* aff. *albomacula* clade C (Donohoo & Gosliner, 2020) are revealed to be a new species of *Avaldesia* with labial rodlets, distinct reproductive characteristics and wide morphological variation. *Avaldesia tamatoa* n. sp. is genetically separated from *A. albomacula*/*A. tahala* by a minimum divergence of 12.0%/9.4% in the COI gene and 4.4%/3.7% in the 16S rRNA gene, respectively. Externally, all three species share a similar background colouration (i.e. predominantly shades of red and brown), while *A. tamatoa* n. sp. and *A. albomacula* also have filamentous tan papillae and a white spot anterior of the gill pouch (always present in *A. albomacula* and occasionally present in *A. tamatoa* n. sp.), and *A. tahala* is more spiculose with large, conical tan papillae. In *A. albomacula*, the filamentous papillae are more numerous, the branchial plume is composed of six tripinnate branches, the rhinophoral lamellae are all one colour (tan or brown) and the rhinophoral sheath is smooth, whereas in *A. tamatoa* n. sp. and *A. tahala*, the dorsum also has low ridging with a complex pattern and numerous tubercles concentrated towards the edge of the dorsum, two-tone rhinophoral lamellae and a scalloped rhinophoral sheath. *Avaldesia tamatoa* n. sp. has longer, white tubercles along the dorsum that are absent in *A. tahala* and the branchial plume is composed of six bipinnate, occasionally tripinnate, branches (Chan & Gosliner, 2007: figs 1C–E; Figs 3, 7, 8).

Internally, the radula of all three species is similar (i.e. simple and hamate with increasing denticulation towards the semi or full fimbriate outermost teeth); however, *A. tamatoa* is unique in possessing small rodlets on the labial cuticle. There are key characteristics in the reproductive systems of the three species that also assist with species identification. The reproductive system of *A. tamatoa* n. sp. includes a bursa copulatrix twice the size of the receptaculum seminis, a granular vestibular gland armed with a hollow hook-shaped vestibular spine and a penis armed with two hook-shaped spines (Figs 5C, 6C, D). In contrast, in *A. tahala*, the bursa is slightly larger than the receptaculum, the vestibular gland is fimbriate and armed with a hollow hook-shaped spine and the penis is armed with one straight/slightly curved spine (Chan & Gosliner, 2007: fig. 2D; Figs 5B, 6B), while in *A. albomacula*, the bursa copulatrix and receptaculum are similar in size, the granular vestibular gland is unarmed and the penis is armed with numerous hook-shaped penial spines (Chan & Gosliner, 2007: fig. 2C; Figs 5A, 6A).

Previously, specimens of *A. tamatoa* n. sp. have been misidentified as *A. albomacula* or *A. tahala* due to overlap in dorsum, rhinophore and branchial plume colouration. This may be attributed to the lack of geographical separation between these three species as all three are found in the central and western Pacific Ocean (Fig. 1). Furthermore, each species exhibits a range of physical colouration; however, *A. tamatoa* n. sp. exhibits the widest range of colouration within *Avaldesia* (Fig. 7). Despite the close similarities between all three species, there are noticeable external differences combined with strong internal and genetic differences that separate *A. tamatoa* n. sp. from *A. albomacula* and *A. tahala* and support its position as a distinct species within *Avaldesia*.

DISCUSSION

The new genus *Avaldesia*, consisting of two previously described species and one new species described here, is genetically distinct from the morphologically similar genus *Thordisa*, as well as other genera within Discodoridae. *Avaldesia albomacula* and *Avaldesia tahala* were originally described as members of *Thordisa* based on morphological characteristics such as large tubercles and papillae on the dorsum, hamate radular teeth, fimbriate outermost radular teeth and a vestibular gland that may be armed with vestibular spines (Chan & Gosliner, 2007). Externally, species of *Avaldesia* exhibit wider morphological colouration with fewer dispersed tubercles, more dorsum papillae, and in *A. tamatoa* n. sp. and *A. tahala* the presence of dorsum ridging. In comparison, species of *Thordisa* are generally more uniform in colour (i.e. cream in *Thordisa aculeata* Ortea & Á. Valdés, 1995; lemon-yellow in *T. aurea* Pruvot-Fol, 1951 and *T. bimaculata*; bright red in *T. nieseni* Chan & Gosliner, 2007; olive green in *T. diuda* Er. Marcus, 1955; brown in *T. azmanii* Cervera & García-Gómez, 1989, etc.) and have a more even distribution of tubercles across the entire dorsum. These tubercles may be very short as seen in *T. bimaculata* or *T. verrucosa* (Crosse, 1864) or larger and longer as seen in *T. villosa* (Alder & Hancock, 1864). The tubercles can also be thin and elongate like those in *T. sanguinea* Baba, 1955 and *T. aculeata*, or more complex as seen in *T. luteola* Chan & Gosliner, 2007 and *T. harrisi* Chan & Gosliner, 2006.

Internally, both genera share a vestigial rachidian fold and a radula composed of simple hamate teeth with fimbriate outermost teeth; however, *Avaldesia* also has similarly sized inner and middle radular teeth as well as denticulation along the outer side of the inner and middle laterals. In *Thordisa*, the inner radular teeth are generally smooth and smaller than the middle and outer teeth with the exception of *T. oliva* and *T. nieseni*, which may have bifurcated tips on the inner teeth and *T. villosa*, which has similarly sized inner and middle teeth (Chan & Gosliner, 2007; Figs 4, 17, 20) that lack denticles. *Thordisa pinguis* (Er. Marcus & Ev. Marcus, 1970) also exhibits denticulation along the inner and middle radular teeth; however, the denticulation is much more pronounced and found on both sides of the radular teeth. Furthermore, the presence of labial armature and fimbriate outermost radular teeth as well as a reproductive system with multiple penial spines, a solid rather than hollow vestibular spine and a narrow vestibular gland suggest that *T. pinguis* is likely a species of *Carminodoris* rather than *Thordisa* or *Avaldesia* (Er. Marcus & Ev. Marcus, 1970: figs 33–38). The illustration of the preserved specimen also indicates that it has densely arranged rounded tubercles, which are more characteristic of species of *Carminodoris* than species of *Thordisa*. To date, no additional specimens of *T. pinguis* have been collected from the type locality in the Society Islands, Tahiti since the original description in 1970. Therefore, we are unable to confirm the placement of *T. pinguis* within Discodoridae using molecular techniques. Individuals identified as *T. setosa* from the Hawaiian Islands also have slightly smaller inner radular teeth with increasing denticulation towards the outermost fimbriate teeth and a reproductive system with a lobate vestibular gland and no penial or vestibular spines indicated (Kay & Young, 1969). In the remarks section of the original description for *A. albomacula*, Chan and Gosliner (2007) make morphological comparisons between *T. setosa* and *A. albomacula* as both species are found in the Hawaiian Islands. They identify a clear separation between the two based on the presence of numerous patches of dark colouration along the mantle of *T. setosa*, which also has a reproductive system with a larger female gland mass and lobate prostate. Additionally, we note that *T. setosa* also lacks penial and vestibular armature, while *A. albomacula* has numerous penial spines and no vestibular spines. *Thordisa setosa* is likely another species of *Avaldesia*; however, additional representatives preserved adequately for molecular sequencing are necessary to make this determination. Furthermore, the reproductive system of this species needs to be re-examined to determine whether penial or vestibular gland spines may have been overlooked.

In both *Thordisa* and *Avaldesia*, the reproductive system includes a vestibular gland (one in *Avaldesia*, none to two in *Thordisa*), which may be armed with one or more vestibular spines; however, the vestibular spines in *Avaldesia* are hollow, whereas the vestibular spines in *Thordisa* are solid. The shape of the vestibular gland also varies. In *Avaldesia*, the vestibular gland is lobate (Fig. 5), while in *Thordisa*, most species have a pouch-shaped vestibular gland as seen in the type species *T. villosa*. However, variation in vestibular gland shape can be seen in *T. filix* Pruvot-Fol, 1951, which has an elongated, coil-shaped vestibular gland, and *T. aculeata*, which has a narrow and elongated vestibular gland. In *Avaldesia*, all three species have an armed penis, while in *Thordisa*, only 5 of *c.* 20 species (*T. bimaculata*, *T. diuda*, *T. filix*, *T. nieseni* and *T. rubescens* Behrens & Henderson, 1981) are known to have penial spines. The relative sizes of the bursa copulatrix and the receptaculum seminis also differ between *Avaldesia* and *Thordisa*. In *Thordisa*, the bursa copulatrix is twice the size of the receptaculum seminis, while in *Avaldesia*, there is more variability. The bursa can be either the same size (*A. albomacula*; Fig. 5A), slightly larger (*A. tahala*; Fig. 5B) or twice the size of the receptaculum seminis (*A. tamatoa* n. sp.; Fig. 5C).

Previous morphological phylogenies suggested *Thordisa* was an intermediary genus between a clade of *Asteronotus*/*Halgerda* and *Hoplodoris* (Valdés, 2002) or the most basal genus when compared with *Asteronotus*, *Halgerda* and *Hoplodoris* (Chan and Gosliner, 2006, 2007). In our molecular analyses, *Thordisa* is more closely related to *Geitodoris*, *Discodoris* and *Carminodoris* than *Avaldesia*, which is part of a separate clade composed of *Taringa* Er. Marcus, 1955, an undescribed group of *Sclerodoris*, *Hoplodoris* and *Asteronotus*. Our results support the study by Donohoo & Gosliner (2020), which suggested that *Avaldesia*, previously identified as *Thordisa* aff. *albomacula* clades A–C, is well supported as the sister taxa to *Hoplodoris* and *Asteronotus*. Morphologically, all three genera share a handful of characteristics, including the presence of large tubercles and papillae along the dorsum, hamate radular teeth and a vestibular gland (i.e. accessory gland in *Hoplodoris* and *Asteronotus*), usually armed with spines. Furthermore, *Hoplodoris* and *Avaldesia* also share the presence of an

armed penis and in the case of *A. tamatoa* n. sp. the presence of jaw rodlets arming the labial cuticle.

Avaldesia is morphologically different enough from *Thordisa* and other discodorid genera to be identified in the field; however, *Avaldesia* species identifications based on external morphology alone may be difficult. Historically, individuals *of A. tamatoa* n. sp. have been misidentified as either *A. albomacula* or *A. tahala* since all three species share a similar biogeographical range and over-lapping colouration (i.e. shades of red, brown, purple, etc.); however, the use of internal characteristics (i.e. size and shape of the vestibular gland, presence/absence of a vestibular spine, number/shape of spines arming the penis, etc.) and molecular data may further assist with *Avaldesia* species identifications. Genera and species identifications within the nudibranch family Discodorididae are notoriously challenging; however, we successfully split the polyphyletic genus *Thordisa* into two and describe a new genus, *Avaldesia*, based on a combination of genetics and morphological data.

ACKNOWLEDGEMENTS

This work was facilitated by several individuals who collected specimens, including Pauline Fiene, Jessica Goodheart, Alicia Hermosillo, Vanessa Knutson, Cory Pittman, Christina Piotrowski, Mohammed Naoufal Tamsouri and the CAS Papua New Guinea Biodiversity 2012 Expedition. The authors also thank Scott and Jeanette Johnson for providing photos and extensive collection information about specimens they collected from the Marshall Islands. The authors also greatly appreciate the help of Lola Bragado Álvarez, Fernando García Guerrero, Isabel Rey and Beatriz Álvarez Dorda from the Museo Nacional de Ciencias Naturales of Madrid for sequencing *Thordisa azmanii* (MNCN 15.05/90803 and MNCN-ADN 151079) on such short notice. This work was supported by an NSF grant DEB 1856407 awarded to T.M.G. for phylogenetic studies of nudibranchs. Support was also provided by the Hope for Reefs collaborative research initiative of CAS. Fieldwork in the Philippines was supported by NSF DEB 1257630 grant to T.M.G., Kent Carpenter, Richard Mooi, Luiz Rocha and Gary Williams and from a generous donation from Will and Margaret Hearst. Material for some species studied here was kindly supported by Dr Philippe Bouchet and the Muséum national d'Histoire naturelle, Paris (MNHN). Specifically, the Madang expedition specimens were obtained during the "Our Planet Reviewed" Papua Niugini expedition organized by MNHN, Pro Natura International, Institut de Recherche pour le Développement and University of Papua New Guinea; principal investigators Philippe Bouchet, Claude Payri and Sarah Samadi. The organizers acknowledge funding from the Total Foundation, Prince Albert II of Monaco Foundation, Fondation EDF, Stavros Niarchos Foundation and Entrepose Contracting and in-kind support from the Divine Word University. The expedition operated under a permit delivered by the Papua New Guinea Department of Environment and Conservation. The authors also appreciate the feedback we received from two anonymous reviewers and the editors at the Journal of Molluscan Studies, which improved this manuscript. This work was supported by the National Science Foundation (DEB 1856407 and DEB 1257630). No animal testing was performed during this study. All necessary permits for sampling and observational field studies have been obtained by the authors from the competent authorities and are mentioned in above, if applicable. The study is compliant with CBD and Nagoya protocols.

SUPPLEMENTARY MATERIAL

Supplementary material is available at *Journal of Molluscan Studies* online.

DATA AVAILABILITY

The genome sequence data that support the findings of this study are available at GenBank (https://www.ncbi.nlm.nih.gov/) under the following accession numbers: OL960075−OL960082, OQ357898, OR088279, OL964389−OL964402, OQ359121, OR096359, OL956540−OL956553, OQ368830, OR089094, OL964405−OL964419 and OQ359122.

REFERENCES

ALDER, J. & HANCOCK, A. 1864. Notice of a collection of nudibranchiate mollusca made in India by Walter Elliot Esq. with descriptions of several new genera and species. *Transactions of the Zoological Society of London*, **5**: 113–147.

ALFARO, M.E., ZOLLER, S. & LUTZONI, F. 2003. Bayes or bootstrap? A simulation study comparing the performance of Bayesian Markov Chain Monte Carlo sampling and bootstrapping in assessing phylogenetic confidence. *Molecular Biology and Evolution*, **20**: 255–266.

ALVIM, J. & PIMENTA, A.D. 2013. Taxonomic review of the family Discodorididae (Mollusca: Gastropoda: Nudibranchia) from Brazil, with descriptions of two new species. *Zootaxa*, **3745**: 152–198.

BABA, K. 1955. *Opisthobranchia of Sagami Bay*. Iwanami Shoten, Toyko.

BEHRENS, D.W. & HENDERSON, R. 1981. Two new cryptobranch dorid nudibranchs from California. *Veliger*, **24**: 120–128.

BERGH, R. 1876. *Malacologische untersuchungen*. Reisen im Archipel der Philippinen. Theil 2, Heft 10. 377–428, plates 49–53, Kreidel, Wiesbaden.

BERGH, R. 1877. *Malacologische untersuchungen*. Reisen im Archipel der Philippinen. Zweiter Theil. Wissenschaftliche Resultate, Band 2, Theil 2, Heft 10. 495–546, plates 58–61**.** Kreidel, Wiesbaden.

BERGH, R. 1878. *Malacologische untersuchungen*. Reisen im Archipel der Philippinen, Vol. 2. pp. 547–601, pls 62–65. Kreidel, Wiesbaden.

BERGH, R. 1880a. *Malacologische untersuchungen*. Reisen im Archipel der Philippinen. Theil 4, Heft 2. 1–78, plates A–F. Kreidel, Wiesbaden.

BERGH, R. 1880b. Beiträge zur kenntniss der japanischen nudibranchien. I. *Verhandlungen der Koniglich-Kaiserlichen Zoologisch-Botanischen Gesellschaft in Wien*, **30**: 155–200.

BERGH, R. 1889. *Malacologische untersuchungen*. Reisen im Archipel der Philippinen. Theil 3, Heft 16. 815–872, plates 82–84. Kreidel, Wiesbaden.

BERGH, R. 1891. Die cryptobranchiaten Dorididen. *Zoologische Jahrbücher, Abteilung für Systematik, Geographie und Biologie der Tiere*, **6**: 103–144.

CAMACHO-GARCÍA, Y.E. & GOSLINER, T.M. 2008. Systematic revision of *Jorunna* Bergh, 1876 (Nudibranchia: Discodorididae) with a morphological phylogenetic analysis. *Journal of Molluscan Studies*, **74**: 143–181.

CERVERA, J.L. & GARCÍA-GÓMEZ, J.C. 1989. A new species of the genus *Thordisa* from the southwestern Iberian Peninsula. *Veliger*, **32**: 382–386.

CHAN, J.M. & GOSLINER, T. 2006. Description of a new species of *Thordisa* (Nudibranchia: Discodorididae) from Panama. *Proceedings of the California Academy of Sciences*, **57**: 981–990.

CHAN, J.M. & GOSLINER, T.M. 2007. Preliminary phylogeny of *Thordisa* (Nudibranchia: Discodorididae) with descriptions of five new species. *Veliger*, **48**: 284–308.

COLGAN, D.J., MCLAUCHLAN, A., WILSON, G.D.F., LIVINGSTON, S.P., EDGECOMBE, G.D., MACARANAS, J., CASSIS, G. & GRAY, M.R. 1998. Histone H3 and U2 snRNA DNA sequences and arthropod molecular evolution. *Australian Journal of Zoology*, **46**: 419−437.

CROSSE, H. 1864. Diagnoses d'espèces nouvelles. *Journal de Conchyliologie*, **12**: 42–43.

DAYRAT, B., TILLIER, A., LECOINTRE, G. & TILLIER, S. 2001. New clades of euthyneuran gastropods (Mollusca) from 28S rRNA sequences. *Molecular Phylogenetics and Evolution*, **19**: 225–235.

DONOHOO, S.A. & GOSLINER, T.M. 2020. A tale of two genera: the revival of *Hoplodoris* (Nudibranchia: Discodorididae) with the description of new species of *Hoplodoris* and *Asteronotus*. *Zootaxa*, **4890**: 1–37.

DRUMMOND, A.J. & RAMBAUT, A. 2007. BEAST: Bayesian evolutionary analysis by sampling trees. *BMC Evolutionary Biology*, **7**: 214.

EHRENBERG, C.G. 1828–1831. Symbolae physicae animalia evertebrata exclusis insectis. Series prima cum tabularum decade prima continent animalia africana et Asiatica. Decas prima. *Symbolae physicae, seu Icones adhue ineditae corporum naturalium novorum aut minus cognitorum, quae ex itineribus per Libyam, Aegyptum, Nubiam, Dengalam, Syriam, Arabiam et Habessiniam Pars Zoologica*, **4**. pls. 1–2 (1828), text (1831). Ex Officina Academica, venditur a Mittlero, Berolini.

FAHEY, S.J. 2003. Phylogeny of *Halgerda* (Mollusca: Gastropoda) based on combined analysis of mitochondrial CO1 and morphology. *Invertebrate Systematics*, **17**: 617–624.

FAHEY, S.J. & GOSLINER, T.M. 1999. Preliminary phylogeny of *Halgerda* (Nudibranchia: Halgerdidae) from the tropical Indo-Pacific, with descriptions of three new species. *Proceedings of the California Academy of Sciences*, **51**: 425–448.

FAHEY, S.J. & GOSLINER, T.M. 2001. The phylogeny of *Halgerda* (Opisthobranchia, Nudibranchia) with the description of a new species from Okinawa. *Zoologica Scripta*, **30**: 199–213.

FAHEY, S.J. & GOSLINER, T.M. 2003. Mistaken identities: on the Discodoridiidae genera *Hoplodoris* Bergh, 1880 and *Carminodoris* Bergh, 1889 (Opisthobranchia, Nudibranchia). *Proceedings of the California Academy of Sciences*, **54**: 169–208.

FOLMER, O., HOEH, W.R., BLACK, M.B. & VRIJENHOEK, R.C. 1994. Conserved primers for PCR amplification of mitochondrial DNA from different invertebrate phyla. *Molecular Marine Biology and Biotechnology*, **3**: 294–299.

FUJISAWA., T. & BARRACLOUGH, T.G. 2013. Delimiting species using single-locus data and the generalized mixed yule coalescent approach: a revised method and evaluation on simulated data sets. *Systematic Biology*, **62**: 707–724.

GAROVOY, J.B., VALDÉS, Á. & GOSLINER, T.M. 2001. Phylogeny of the genus *Rostanga* (Nudibranchia), with descriptions of three new species from South Africa. *Journal of Molluscan Studies*, **67**: 131–144.

GIRIBET, G., OKUSU, A., LINDGREN, A.R., HUFF, S.W., SCHRÖDL, M. & NISHIGUCHI, M.K. 2006. Evidence for a clade composed of molluscs with serially repeated structures: monoplacophorans are related to chitons. *Proceedings of the National Academy of Sciences of the USA*, **103**: 7723–7728.

GÖBBELER, K. & KLUSSMANN-KOLB, A. 2010. Out of Antarctica?—New insights into the phylogeny and biogeography of the pleurobranchomorpha (Mollusca, Gastropoda). *Molecular Phylogenetics and Evolution*, **55**: 996–1007.

GOSLINER, T.M., BEHRENS, D.W. & VALDÉS, Á. 2008. *Indo-Pacific nudibranchs and sea slugs: a field guide to the world's most diverse fauna*. Sea Challengers, California Academy of Sciences, San Franscisco, CA.

GOSLINER, T.M., VALDÉS, Á. & BEHRENS, D.W. 2015. *Nudibranch and sea slug identification; Indo-Pacific*. New World Publications, Inc., Jacksonville, FL.

GOSLINER, T.M. & VALDÉS, Á. 2002. Sponging off of Porifera: new species of cryptic dorid nudibranchs (Mollusca, Nudibranchia) from the tropical Indo-Pacific. *Proceedings of the California Academy of Sciences*, **53**: 51–61.

GOSLINER, T.M., VALDÉS, Á. & BEHRENS, D.W. 2018. *Nudibranch and sea slug identification; Indo-Pacific*. New World Publications, Inc., Jacksonville, FL.

HALLAS, J.M., CHICHVARKHIN, A. & GOSLINER, T.M. 2017. Aligning evidence: concerns regarding multiple sequence alignments in estimating the phylogeny of the Nudibranchia suborder Doridina. *Royal Society Open Science*, **4**: 171095.

INNABI, J., STOUT, C.C. & VALDÉS, Á. 2023. Seven new "cryptic" species of Discodoridiidae (Mollusca, Gastropoda, Nudibranchia) from New Caledonia. *ZooKeys*, **1152**: 45–95.

KATOH, K., ASIMENOS, G. & TOH, H. 2009. Multiple alignment of DNA sequences with MAFFT. In: *Bioinformatics for DNA sequence analysis*. (D. Posada, ed.), pp. 39–64. Humana Press, New York.

KAY, E.A. & YOUNG, D.K. 1969. The Doridacea (Opisthobranchia; Mollusca) of the Hawaiian Islands. *Pacific Science*, **23**: 172–231.

KEARSE, M., MOIR, R., WILSON, A., STONES-HAVAS, S., CHEUNG, M., STURROCK, S., BUXTON, S., COOPER, A., MARKOWITZ, S., DURAN, C. & THIERER, T. 2012. Geneious Basic: an integrated and extendable desktop software platform for the organization and analysis of sequence data. *Bioinformatics*, **28**: 1647–1649.

KEKKONEN, M., MUTANEN, M., KAILA, L., NIEMINEN, M. & HEBERT, P.D. 2015. Delineating species with DNA barcodes: a case of taxon dependent method performance in moths. *PLoS One*, **10**: e0122481.

LANCE, J.R. 1966. New distributional records of some northeastern Pacific Opisthobranchiata (Mollusca: Gastropoda) with descriptions of two new species. *Veliger*, **9**: 69–81.

LANFEAR, R., FRANDSEN, P.B., WRIGHT, A.M., SENFELD, T. & CALCOTT, B. 2017. PartitionFinder 2: new methods for selecting partitioned models of evolution for molecular and morphological phylogenetic analyses. *Molecular Biology and Evolution*, **34**: 772–773.

LINDSAY, T., KELLY, J., CHICHVARKHIN, A., CRAIG, S., KAJIHARA, H., MACKIE, J. & VALDÉS, Á. 2016. Changing spots: pseudocryptic speciation in the North Pacific dorid nudibranch *Diaulula sandiegensis* (Cooper, 1863) (Gastropoda: Heterobranchia). *Journal of Molluscan Studies*, **82**: 564–574.

MADDISON, W.P. & MADDISON, D.R. 2018. Mesquite: a modular system for evolutionary analysis (Version 3.31). Avavailable at: http://mesquiteproject.org. (1 August 2022, date last accessed).

MARCUS, E.R. 1955. Opisthobranchia from Brazil. *Boletim da Facultade de Filosofia, Ciências e Letras da Universidade de São Paulo, Zoologia*, **20**: 89–261, plates 1–30.

MARCUS, E.R. & MARCUS, E.V. 1970. Opisthobranch mollusks from the southern tropical Pacific. *Pacific Science*, **24**: 155–179.

MARCUS, E.V. & MARCUS, E.R. 1963. Opistobranchs from the Lesser Antilles. *Studies on the Fauna of Curaçao and Other Caribbean Islands: no 79*, **19**: 1–76.

MARTÍN-HERVÁS, M.D.R., CARMONA, L., MALAQUIAS, M.A.E., KRUG, P.J., GOSLINER, T.M. & CERVERA, J.L. 2021. A molecular phylogeny of *Thuridilla* Bergh, 1872 sea slugs (Gastropoda, Sacoglossa) reveals a case of flamboyant and cryptic radiation in the marine realm. *Cladistics*, **37**: 647–676.

MOLLUSCABASE EDS. 2021. MolluscaBase. Discodoridiidae Bergh, 1891. Avavailable at: http://molluscabase.org/aphia.php?p=taxdetails&id=1761. (31 January 2023, date last accessed).

MÜLLER, O.F. 1776. *Zoologia Danica, Seu, Animalium Daniae et Norvegiae Rariorum ac Minus Notorum Descriptiones Et Historia*. Hauniae et Lipsiae: Sumtibus Weygandinis, Copenhagen.

NEUHAUS, J., RAUCH, C., BAKKEN, T., PICTON, B., POLA, M. & MALAQUIAS, M.A.E. 2021. The genus *Jorunna* (Nudibranchia: Discodoridiidae) in Europe: a new species and a possible case of incipient speciation. *Journal of Molluscan Studies*, **87**: eyab028.

NIMBS, M.J., LARKIN, M., DAVIS, T.R., HARASTI, D., WILLAN, R.C. & SMITH, S.D. 2016. Southern range extensions for twelve heterobranch sea slugs (Gastropoda: Heterobranchia) on the eastern coast of Australia. *Marine Biodiversity Records*, **9**: 1–12.

NIMBS, M.J. & SMITH, S.D. 2017. An illustrated inventory of the sea slugs of New South Wales, Australia (Gastropoda: Heterobranchia). *Proceedings of the Royal Society of Victoria*, **128**: 44–113.

ORTEA, J. & VALDÉS, Á. 1995. Una nueva especie de *Thordisa* Bergh, 1877 (Mollusca: Nudibranchia: Discodoridiidae) de las costas de Angola. *Avicennia*, **3**: 35–41.

PADULA, V., BAHIA, J., STÖGER, I., CAMACHO-GARCÍA, Y., MALAQUIAS, M.A.E., CERVERA, J.L. & SCHRÖDL, M. 2016. A test of colour-based taxonomy in nudibranchs: molecular phylogeny and species delimitation of the *Felimida clenchi* (Mollusca: Chromodoridiidae) species complex. *Molecular Phylogenetics and Evolution*, **103**: 215–229.

PADULA, V. & VALDÉS, A. 2012. Phylogeny and biogeography of *Paradoris* (Nudibranchia, Discodoridiidae), with the description of a new species from the Caribbean Sea. *Veliger*, **51**: 165–176.

PALUMBI, S.R., MARTIN, A.P., ROMANO, S., MCMILLAN, W.O., STICE, L. & GRABOWSKI, G. 1991. *The simple fool's guide to PCR*. Special Publication, Department of Zoology, University of Hawaii, Honolulu, Hawaii.

PEASE, W.H. 1860. Descriptions of new species of Mollusca from the Sandwich Islands. *Proceedings of the Zoological Society of London*, **28**: 18–36.

PLATT, A.R., WOODHALL, R.W. & GEORGE JR, A.L. 2007. Improved DNA sequencing quality and efficiency using an optimized fast cycle sequencing protocol. *Biotechniques*, **43**: 58–62.

PONS, J., BARRACLOUGH, T.G., GOMEZ-ZURITA, J., CARDOSO, A., DURAN, P., HAZELL, S., KAMOUN, S., SUMLIN, W.D. & VOGLER, A.P. 2006. Sequence-based species delimitation for the DNA taxonomy of undescribed insects. *Systematic Biology*, **55**: 595–609.

PRUVOT-FOL, A. 1951. Etudes des nudibranches de la Méditerranée 2. *Archives de Zoologie Expérimentale et Générale*, **88**: 1–80.

PUILLANDRE, N., BROUILLET, S. & ACHAZ, G. 2021. ASAP: assemble species by automatic partitioning. *Molecular Ecology Resources*, **21**: 609–620.

PUILLANDRE, N., LAMBERT, A., BROUILLET, S. & ACHAZ, G.J.M.E. 2012. ABGD, automatic barcode gap discovery for primary species delimitation. *Molecular Ecology*, **21**: 1864–1877.

RISBEC, J. 1928. Contribution à l'étude des nudibranches néo-calédoniens. *Faune des Colonies Françaises*, **2**: 1–328, figs. 1–98, pls. 1–12.

RONQUIST, F. & HUELSENBECK, J.P. 2003. MrBayes 3: Bayesian phylogenetic inference under mixed models. *Bioinformatics*, **19**: 1572–1574.

SØRENSEN, C., RAUCH, C., POLA, M. & MALAQUIAS, M. 2020. Integrative taxonomy reveals a cryptic species of the nudibranch genus *Polycera* (Polyceridae) in European waters. *Journal of the Marine Biological Association of the United Kingdom*, **100**: 733–752.

STAMATAKIS, A. 2014. RAxML version 8: a tool for phylogenetic analysis and post-analysis of large phylogenies. *Bioinformatics*, **30**: 1312–1313.

TIBIRIÇÁ, Y., POLA, M. & CERVERA, J.L. 2018. Systematics of the genus *Halgerda* Bergh, 1880 (Heterobranchia: Nudibranchia) of Mozambique with descriptions of six new species. *Invertebrate Systematics*, **32**: 1388–1421.

TIBIRIÇÁ, Y., STRÖMVOLL, J. & CERVERA, J.L. 2023. Can you find me? A new sponge-like nudibranch from the genus *Jorunna* Bergh, 1876 (Mollusca, Gastropoda, Discodorididae). *Zoosystematics and Evolution*, **99**: 63–75.

VALDÉS, Á. 2002. A phylogenetic analysis and systematic revision of the cryptobranch dorids (Mollusca, Nudibranchia, Anthobranchia). *Zoological Journal of the Linnean Society*, **136**: 535–636.

YONOW, N. 2015. Sea slugs: unexpected biodiversity and distribution. In: *The red sea*. (N.M.A. Rasul & I.C.F. Stewart, eds), pp. 531–550. Springer, Berlin.

ZHANG, J., KAPLI, P., PAVLIDIS, P. & STAMATAKIS, A. 2013. A general species delimitation method with applications to phylogenetic placements. *Bioinformatics*, **29**: 2869–2876.